JAERI - M
90-014

THE TRANSVERSE STRESS EFFECT ON THE CRITICAL CURRENT OF JELLY-ROLL MULTIFILAMENTARY Nb_3Al WIRES

February 1990

Dimitris ZERITIS*

日 本 原 子 力 研 究 所
Japan Atomic Energy Research Institute

JAERI-Mレポートは，日本原子力研究所が不定期に公刊している研究報告書です。
入手の問合わせは，日本原子力研究所技術情報部情報資料課（〒319-11茨城県那珂郡東海村）あて，お申しこしください。なお，このほかに財団法人原子力弘済会資料センター（〒319-11 茨城県那珂郡東海村日本原子力研究所内）で複写による実費頒布をおこなっております。

JAERI-M reports are issued irregularly.
Inquiries about availability of the reports should be addressed to Information Division, Department of Technical Information, Japan Atomic Energy Research Institute, Tokai-mura, Naka-gun, Ibaraki-ken 319-11, Japan.

編集兼発行　日本原子力研究所
印　　刷　㈱原子力資料サービス

JAERI-M 90-014

The Transverse Stress Effect on the Critical Current of Jelly-roll Multifilamentary Nb_3Al Wires

Dimitris ZERITIS*

Department of Thermonuclear Fusion Research
Naka Fusion Research Establishment
Japan Atomic Energy Research Institute
Naka-machi, Naka-gun, Ibaraki-ken

(Received January 22, 1990)

Experiments were conducted to determine the transverse stress sensitivity of the critical current of jelly-roll multifilamentary Nb_3Al wires, primarily at 12T but also at other magnetic fields. For comparison, similar experiments were conducted on bronze-process Ti-alloyed multifilamenary Nb_3Sn wires. In total four samples were experimented upon, two jelly-roll Nb_3Al samples of 0.8 mm and 1.03mm diameter, respectively, one bronze-process Nb_3Sn sample of 1.0mm diameter, and one internally-stabilized bronze-process Nb_3Sn sample of 1.09mm diameter. As was expected, the Nb_3Al samples proved vastly superior to the Nb_3Sn samples with regard to transverse compressive stress, exhibiting significant I_c-degradation for transverse stresses above 100MPa. At 12T and at 150MPa of transverse compression - conditions expected in fusion magnets - the 0.8mm-diameter sample exhibited an I_c-degradation of ~20%, whereas the 1.03mm-diameter sample of ~28%. Under the same conditions, the 1.0mm-diameter Nb_3Sn sample exhibited an I_c-degradation of ~65%, whereas at 12T and 120MPa the 1.09mm-diameter Nb_3Sn sample exhibited an I_c-degradation also of ~65%. However, the measured non-copper critical current densities at high magnetic fields of the Nb_3Al samples were lower than those of the Nb_3Sn samples. Further development is needed to improve this aspect of their performance, nevertheless there is optimism that Nb_3Al will eventually become a useful superconductor for large-scale, high-field applications.

Keywords: Superconductors, Nb_3Al, Nb_3Sn, Jelly-roll, Transverse Stress Effect, Critical current

---

* Massachusetts Institute of Technology

ジェリー・ロール型多芯Nb_3Al導体の臨界電流値への横圧縮効果

日本原子力研究所那珂研究所核融合研究部
Dimitris ZERITIS*

（1990年1月22日受理）

高磁界用超電導材料は現在Nb_3Snが主流であるが，この材料は機械的に弱いという欠点がある。そこで，この材料より機械的特性の優れているNb_3Alに着目して，その臨界電流値への横圧縮効果を，8テスラから15テスラの磁界において研究を行った。サンプルは，ジェリー・ロール法により製作され，比較のためブロンズ法により製作されたNb_3Sn導体についても測定を行った。本研究におけるサンプルは，Nb_3Al 2種類，Nb_3Sn 2種類 合計4種類である。

予想されたように，Nb_3Alの方が100MPa以上の圧力下において臨界電流値の劣化が著しく小さく，機械的特性が優れているという結果が得られた。しかしながら現在のところ，高磁界における臨界電流密度は，Nb_3Snの方がNb_3Alより大きいので，今後の開発研究においてNb_3Alの臨界電流密度の改良が要求される。

本研究の結果より，Nb_3Alは将来において核融合のような大型でかつ高磁界への応用に対して有効な超電導材料となることが示された。

那珂研究所：〒311－01　茨城県那珂郡那珂町大字向山801－1
＊マサチュセッツ工科大学（MIT）

Contents

目　　次

1. Introduction

Magnet technology has advanced considerably in the past years, by dint of the advantages offered by superconductivity. Every advance however has come at the price of having to solve a number of quite difficult technological problems. Every new discovery has meant having to stand up to the demands born from its very promise, nevertheless the engineering world has so far responded with outstanding success. Thousands of large and small superconducting magnets are in routine operation throughout the globe, and doubtless their number will increase in the future.

Currently a major area of technological research involving superconducting magnets is the construction of fusion powerplants, as witnessed by several projects underway in Japan, the United States, Europe, and the Soviet Union. Superconducting magnets are essential to fusion reactors by virtue of their ability to produce plasma-confining magnetic fields. It is estimated however that these superconducting magnets will represent a sizeable fraction of the total capital cost of a fusion powerplant. Moreover their performance will affect both the plasma and the plasma density, so there exists justifiably an urgent need to develop superconducting materials that will boost the performance-limits of the magnets.

Presently the most popular superconductor for applications in magnet technology is NbTi, mainly because it is easily fabricated and may co-processed with copper, but also because it may sustain ductile deformation without significant harm to its superconducting properties. For high-field applications (>12T), superconductors of the A15 family such as Nb_3Sn and Nb_3Al are better suited than NbTi. Of the former Nb_3Sn is widely accepted as the dominant high-field superconductor and is commercially available in a variety of multifilamentary configurations. The main disadvantage of Nb_3Sn is its brittleness and the excessive degradability of its superconducting properties by stress and strain. The equally brittle Nb_3Al on the other hand, though currently not as highly developed as Nb_3Sn and hence not capable of Nb_3Sn's critical current densities in mulfifilamentary wire form, possesses the redeeming quality of significantly lower sensitivity to stress and strain.

In this paper we present for the first time results regarding the transverse stress sensitivity of the critical current of Nb_3Al

multifilamentary wires fabricated by the jelly-roll process. For comparison, we present results from Nb_3Sn multifilamentary wires fabricated in two different geometries by the bronze diffusion process. We examine our findings from a phenomenological standpoint, and set the basis for a theoretical analysis later to follow.

2. Fabrication processes for Nb_3Sn and Nb_3Al wires

The processes whereby superconducting wires are manufactured should be of special interest to the magnet designer. The successful production of a superconducting wire by a certain process will involve a sensitive balance among often conflicting parameters. Altering one parameter may strengthen one aspect of the performance of the wire, yet at the same time it may cause another to deteriorate. In general a certain process for producing a wire involving a specific superconducting compound will have its own special strength, or strengths, as well as its own corresponding weaknesses.

In trying to understand the transverse stress effect, which as we shall show is exhibited by both Nb_3Sn and Nb_3Al wires, knowledge of the fabrication aspects and the metallurgy of these wires will yield useful information.

2.1 Niobium-tin

2.1.1 Metallurgy and superconducting properties

Niobium-tin is an intermetallic compound with a precise stoichiometric composition, Nb_3Sn. The crystallographic structure of Nb_3Sn is of the A15 type, consisting of a body-centered-cubic lattice of Sn atoms with two Nb atoms on each face of the cube. This structure enhances the proximity of the Nb atoms in comparison with elemental niobium, yielding excellent superconducting properties. Pure strain-free Nb_3Sn has an upper critical field at zero temperature of ~28T, and a critical temperature of 18.5K.

In practical wires Nb_3Sn exhibits somewhat degraded critical properties. One reason is the absence of perfect stoichiometric uniformity within the superconducting portion of the wire. Another is the presence of a tetragonal (non-A15) phase of the stoichiometric compound. Another is mechanical stress. In general mechanical stress induces strains in the Nb_3Sn layers of a wire, distorting the A15 phase from the optimal cubic configuration to suboptimal tetragonal configurations. The primary effect of this is to depress B_{c2} and T_c, which in turn leads to a depression in J_c.

The fabrication of practical Nb_3Sn conductors is characterized by

problems stemming from the mechanical properties of Nb_3Sn. Like all other A15 compounds. Nb_3Sn is hard and brittle. Consequently, practical multifilamentary conductors are fabricated not by conventional but by specialized techniques, such as the ones described below[1,4]. Below we emphasize the bronze process, since the Nb_3Sn samples in our experiments were manufactured by that very technique. For the sake of completeness we also mention variants of the bronze process, in an effort to shed some light into the more elusive influences of metallurgy on such macroscopic mechanical effects as the transverse stress effect.

2.1.2 The bronze or internal diffusion process

The fabrication of multifilamentary Nb_3Sn composite conductors became possible with the invention of the bronze process, whereby Nb_3Sn is precipitated via a solid state reaction. The bronze process was discovered independently by three metallurgists in three different countries at the same time: K. Tachikawa[8] at the National Research Institute for Metals in Japan, A.R. Kaufmann[7] at the Whittaker Corporation in the USA, and E.W. Howlett[6] at the Atomic Energy Research Establishment at Hartwell in Great Britain. It is as follows:

Cylinders of pure niobium are inserted in a matrix of copper-tin bronze, and then extruded and drawn down to the final diameter of the wire. The wire is then subjected to a prolonged heat treatment, typically at around 700°C for 1-10 days. During heat treatment tin diffuses through the bronze and reacts with the niobium. Formation of the unwanted Nb_6Sn_5 and $NbSn_2$ phases is suppressed by the copper and thus only Nb_3Sn is formed. All constituents remain in the solid phase throughout the heat treatment, so the filamentary structure of the wire is preserved. Optimization of the heat treatment is usually a compromise between good stoichiometry for high B_{c2} and T_c, and fine grain size for good flux pinning strength. High temperatures and long times result in good stoichiometry, however they are likely to produce large grain sizes.

For high overall current densities it is desirable to maximize the volumetric proportion of Nb_3Sn in the composite. However the metallurgical properties of bronze impose an upper limit on this proportion. The maximum attainable concentration of tin in the ductile α phase bronze is ~13wt.%, whereas the maximum effective concentration ~10wt.%. It is believed nonetheless that filaments containing an

unreacted niobium core have better mechanical properties than fully-reacted ones. Typically, therefore, the proportion of niobium in the composite is adjusted such that a fraction of it, usually ~25 percent, remains unreacted. In view of these considerations the maximum achievable volumetric concentration of Nb_3Sn in the composite is ~25 percent. This is disadvantageous in that the bronze matrix surrounding the Nb_3Sn filaments, of tin concentration approximately ~3wt.% and of resistivity around $\sim 6\times10^{-8}$ Ωm, is useless for stabilization and protection purposes.

Pure copper is usually added to bronze-process Nb_3Sn composites for the interests of stability and quench protection. Copper may be added either externally in the form of a jacket, or internally as the core of the superconducting wire. In either case the copper must be protected from contamination by tin, which may spoil its high conductivity at low temperatures. A thin diffusion barrier, for example tantalum or niobium, is usually interposed between the copper and the bronze.

Many variants of the bronze process have been introduced in order to eliminate or reduce some of the difficulties inherent in it. Many seek to avoid drawing down bronze, which is a difficult process involving many anneals to remove work-hardening. They are briefly reviewed below. Figure 2.1 presents schematically each of these processes.

2.1.3 The deposition or external diffusion process

This process was introduced by Suenaga and Clark[4,5] soon after the discovery of the bronze process. A composite of pure copper with niobium cores is drawn down to the final diameter of the wire. At the final wire size the composite is coated by a thin layer of tin. The composite is subsequently subjected to a low-temperature heat treatment to diffuse the tin into the composite. Thereafter the temperature is raised to promote reaction.

The main advantage of this technique over the original bronze process is that the niobium-copper composite can be drawn to a small size without intermediate anneals. An additional one is that the concentration tin in the matrix is not limited to ~13wt.% as in the case of the bronze process. Thus higher critical current densities are achievable by this process.

The main disadvantage of this process involves the step where tin is diffused into the copper matrix. The outer layer of the wire suffers from delamination for relatively thick layers of plated tin. The delamination problem may be improved by intermediate heat treatments, nevertheless it cannot be completely eliminated. This places limits on the maximum size of the final wire.

There is an additional disadvantage that places limits on the applicability of wires made by the external diffusion process. Conductors may not be produced with a tantalum or niobium diffusion barrier and external copper stabilization. However in conductors employing braided cables, this limitation may not be a major problem since special wires for stabilization, for example tantalum-sheathed copper wires, may be braided together with the superconducting ones. Moreover braids usually require wires of small diameter, therefore the size limitation of wires produced by the external diffusion technique might not be a problem.

2.1.4 The internal tin process

In 1974 a new variant of the bronze process was reported by Hashimoto et al.[10,11]. This process consists of assembling copper-clad niobium rods in a copper billet with a hole in the center. In the center hole is inserted either a copper-clad tin-rich bronze rod, or a copper-clad pure-tin rod. In the latter case an intermediate heat treatment step is required to diffuse the tin into the copper sheath to form the tin-rich alloy. The entire assembly is then cold-drawn to final size for heat treatment to form Nb_3Sn.

As in the case of the external diffusion process, the main advantage of this technique over the bronze process is the elimination of the intermediate annealing steps. However the internal tin process has the advantage of external copper stabilization over the external diffusion process, since the tin is concentrated at the center of the wire as opposed to the outer surface of it. Nevertheless the tin concentration in the matrix is limited and may not be as high as in the external diffusion process. Another possible limitation of this process with regard to large-scale applications is the maximum length of wire that may be fabricated from a single billet. A large billet may not be extruded without melting the tin-rich alloy at its center.

2.1.5 The internal bronze and the niobium tube process

In 1975 two similar modifications to the bronze process were proposed[12,13]. Both of these employ niobium tubes instead of rods. According to the first one, known as the internal bronze process, bronze rods are inserted in copper-clad niobium tubes. A number of these units are assembled in a copper billet for extrusion and drawing. According to the second one, known simply as the tube process, a tin-rich bronze rods, or a pure-tin rod, is first jacketed by copper and then inserted into a copper-clad niobium tube. A number of these units are assembled in a copper billet for extrusion and drawing. At the final wire size, the wire is subjected to heat treatment to form Nb_3Sn.

Particular to the tube process is the separation of the niobium tube from the tin-rich bronze by a layer of copper. The reason for this is that copper suppresses the formation of Nb_6Sn_5 and $NbSn_2$, usually resulting from contact between niobium and tin-rich bronzes. Copper also eliminates the likelihood of large grain sizes that might result from a liquid-phase reaction. Nb_3Sn conductors manufactured by the tube process possess the highest known overall critical current densities at high magnetic fields. The reason behind the high J_c's is the relatively high proportion of stoichiometric Nb_3Sn in the superconducting section of the wire, made possible by the high concentrations of tin that may be diffused during reaction from the tin-rich bronze cores to the niobium tubes.

The common advantage of the internal bronze process and the tube process over the bronze process is that the niobium acts as an automatic diffusion barrier for tin. The addition of tantalum or niobium on the outside surface of the composite is thus unnecessary. Moreover, in contrast with other processes, all of the Nb_3Sn layers are very close to the copper stabilizer. On the other hand, the common disadvantage of both these processes is that the minimum filament size tends to be relatively large, leading to high ac losses when the wires are placed in time-varying magnetic fields.

2.2 Niobium-aluminum

2.2.1 Metallurgy and superconducting properties

In 1958 Wood et al.[17] discovered that the intermetallic A15 compound

Nb_3Al was superconducting with a critical temperature of 17.5K. Thereafter Willens et al.[16] measured a T_c of 18.8K in samples of Nb_3Al made from mixed compacted powders, whereas in 1971 Foner et al.[14,15] measured a critical field of 30T at 4.2K. In 1980 Jorda et al.[29] reported a T_c for Nb_3Al as high as 19.1K.

The superior B_c versus T_c characteristics of bulk Nb_3Al in comparison with those of bulk Nb_3Sn and NbTi are shown in Fig. 2.2 The high B_{c2} and T_c, and also the remarkably high critical current densities attainable by Nb_3Al, justified efforts to manufacture multifilamentary wire. Bevk & Lo[18] were the first to measure the critical current density of Nb_3Al, and reported values greater than $10^4 A/mm^2$ at 20T.

The formation of Nb_3Al is a difficult process, consequently the development of Nb_3Al multifilamentary wires has followed a path different from Nb_3Sn[9,30]. In contrast to Nb_3Sn, the Nb_3Al phase cannot be formed by an equivalent of the bronze diffusion process. The presence of stable ternary phases such as Nb_2CuAl (μ phase) and $Nb(Cu,Al)_2$ (C14 Laves phase) excludes the formation of the A15 phase, as shown by Hunt & Rahman[19]. The only possible way toward the formation of the A15 phase, is by direct interaction of pure niobium and aluminum at temperatures in excess of 1400°C. Such temperatures however are not suitable for industrial wire fabrication, due to the necessary presence of Cu for stabilization. Below 1000°C Nb_3Al must be formed by a nonequilibrium process, but at these low temperatures the two other intermetallic compounds, Nb_2Al and $NbAl_3$, are more stable than Nb_3Al.

Ceresara et al.[21,22] discovered that such a nonequilibrium process may be induced upon reducing the Nb dimensions to submicron sizes. Bormann et al.[20] have shown on Nb-Al multilayers that necessary to the precipitation of Nb_3Al below 1000°C is the intermediate formation of a metastable body-centered-cubic solid-solution containing up to 28at.% Al. If the niobium layers are sufficiently thin, the supersaturated body-centered-cubic phase transforms into the A15 phase, thus excluding the formation of $NbAl_3$.

In recent years there have been important advances in the fabrication of Nb_3Al multifilamentary wires, all of which have aimed to deform the niobium filaments to sufficiently small dimensions so as to promote the nonequilibrium formation of Nb_3Al. Such methods include powder metallurgical processing, and the jelly-roll (or swiss-roll) process.

Below we briefly review the jelly-roll process.

2.2.2 The jelly-roll process

As was mentioned above, when aluminum and niobium are brought into intimate contact on a sufficiently fine scale, useful quantities of Nb_3Al may be formed from a nonequilibrium reaction at temperatures below 1000°C. Ceresara et al.[21,22] employed this fact to develop the jelly-roll process for producing multifilamentary Nb_3Al composites. As such, each unreacted filament consists of a copper-cored "jelly-roll" of alternate superimposed layers of niobium and aluminum. Each of these structures is inserted into a tubular copper container, and then the container is brought to a hexagonal shape. Combining a certain number of these hexagons and after extrusion and drawing, a final unreacted multifilamentary wire may be obtained.

Alternately, as shown in Fig. 2.3, a suitable number of "jelly-rolls" may be assembled into a single extrusion billet. Also, it is often advantageous to wrap ~2-3 layers of niobium between the jelly-roll and the core, and ~3-4 layers of niobium on the outside surface of the jelly-roll before insertion into the billet. The niobium acts as a diffusion barrier against the contamination of copper by aluminum.

At final wire size, the niobium and aluminum layers are ~0.8 and ~0.2μm thick, respectively. In addition to the thickness of the niobium layer, critical to the jelly-roll method is the thickness of the aluminum layer before reaction. Nearly stoichiometric Nb_3Al with good superconducting properties may be precipitated provided that the thickness of the aluminum layer is on the order of ~0.2μm, otherwise phases with poor properties will emerge. By keeping the quantity of aluminum below the stoichiometric ratio, it seems that the formation of unwanted Al-rich compounds may be suppressed. Heat treatment times of a few hours at temperatures ranging from 750°C to 850°C are sufficient to react the layers completely.

Advantages of the jelly-roll process include the absence of intermediate anneals and homogenization heat treatments during mechanical processing, and also the resulting uniform distribution of niobium and aluminum throughout the cross section of the unreacted wire. A Disadvantage of the jelly-roll process pertains to the requirement for heavy mechanical work on the composite billet, to reduce the final thickness of the aluminum layer to very small values for the interests

of high J_c, and also to produce wire in significant lengths. Niobium with high oxygen content may not withstand heavy mechanical work, and this often results in filament breakage and in suboptimal critical current performance.

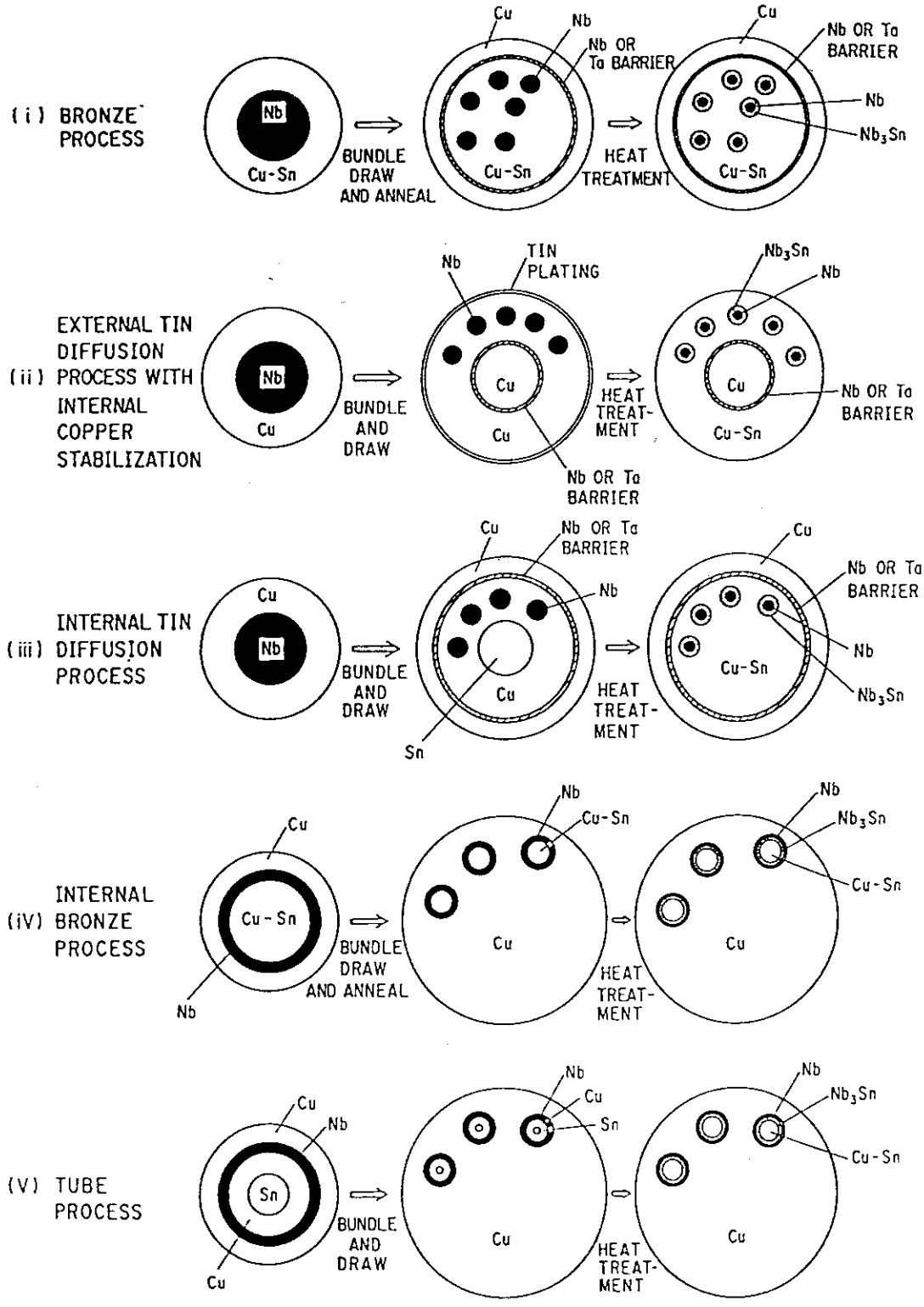

Fig. 2.1 Several bronze-process-based techniques for producing multifilamenatary Nb_3Sn wires

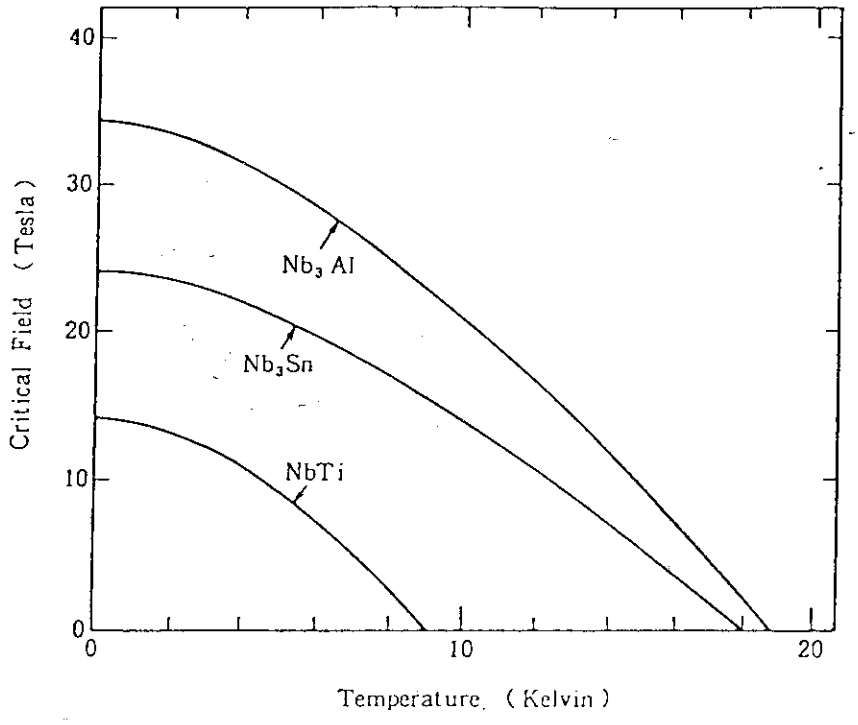

Fig. 2.2 Nb_3Al has a higher upper-critical magnetic field, B_{C2}, and a higher critical temperature, T_C, than Nb_3Sn and NbTi[3]

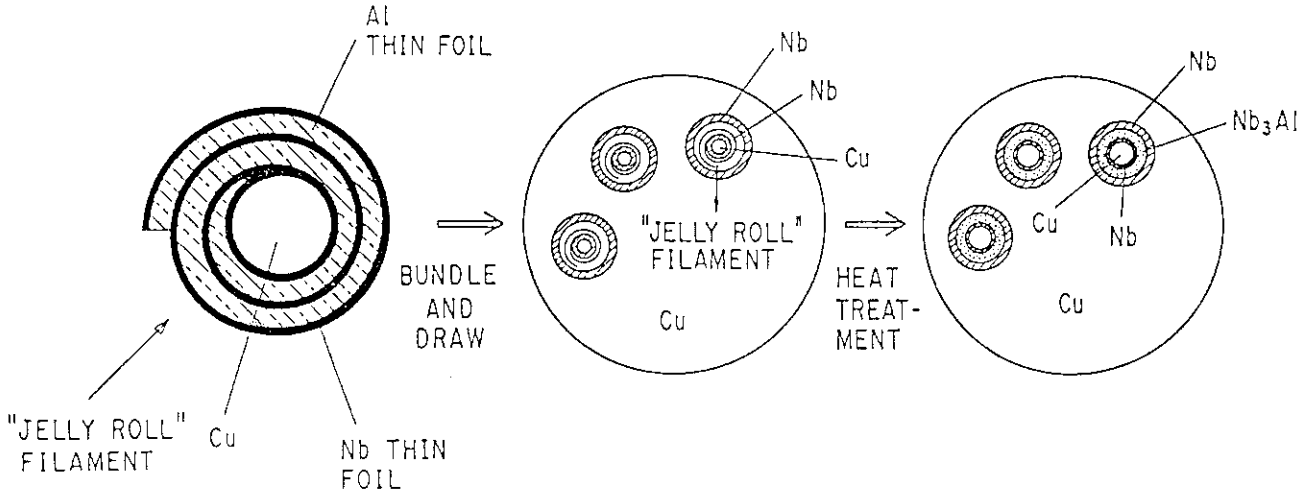

Fig. 2.3 The jelly-roll process for manufacturing multifilamentary Nb_3Al wires

3. The strain effect on the critical current of multifilamentary Nb_3Sn and Nb_3Al superconductors

The stress dependence of the critical current of superconductors was first observed in 1963 by Müller and Saur[23] in thin films of Nb_3Sn and V_3Ga, and in 1964 by Beuheler and Levinstein[24] in monofilamentary Nb_3Sn wires. The first measurements on the reversible nonhydrostatic strain effect were reported in 1975 by Ekin, Fickett and Clark[34], based on experiments on commercial multifilamentary NbTi conductor. The considerably stronger strain dependence of the critical current of multifilamentary Nb_3Sn wires was ascertained the following year, by Ekin[35], Easton and Schwall[25], and McDougall[26]. It has been since established that superconductors of the A15 type, despite their high performance, are unusually susceptible to degradation of their critical properties by stress and strain.

Originally the strain effect the critical properties of A15 superconductors was considered only in the direction of a wire's axis. Currently however, it is understood that transverse stresses can severely degrade the critical properties of A15 superconductors. In today's large-scale, high-field magnets intended for such applications as tokamak fusion, mechanical loads capable of inducing significant axial as well as transverse stresses are abundant. Below we survey the sources of such loads, and then we present briefly the finer points of the axial and the transverse stress effects.

3.1 Sources of mechanical loads in magnets

Mechanical loads in magnets mainly arise from three sources[39]:

(1) Winding tension and bending strain, introduced during the fabrication of a superconducting wire.

(2) Differential thermal contraction between different materials in the magnet structure (support materials, superconductor, etc.), after cooldown to cryogenic temperatures. Thermal mismatches of this sort can introduce significant stresses on magnet conductors, depending on the contraction coefficients. In superconducting composites employing compound superconductors (Nb_3Sn, Nb_3Al etc.), additional internal

stresses can be introduced to the conductor during cooldown from reaction temperatures to cryogenic temperatures. The thermal contraction of the matrix material is greater than that of the superconducting reaction layer, resulting in a precompression of the latter often of as much as 1 percent.

(3) The Lorenz force, experienced by the superconductor when the magnet is energized. The Lorenz force, of considerable magnitude in large-scale, high-field magnets, subjects the conductor to three dimensional stresses. In an unsupported solenoidal magnet, for example, the radial Lorenz force gives rise to hoop stresses in the conductor which cause it to be strained axially. Hoop stresses, in turn, compress the magnet winding radially, subjecting the conductor to transverse compressive stresses. The hoop stress on the overall conductor of a solenoid is given by $\sigma_{hoop}=JBR$, where J is the overall current density in the conductor, B is the magnetic field, and R is the radius of the winding. The transverse stress, acting in the direction perpendicular to both the current and the field, is given by $\sigma_t=JBt$, where t is the thickness of the conductor.

Below we examine the axial and the transverse stress effect on the critical current of A15 superconductors. We do so by looking at Nb_3Sn, currently the most studied and most advanced of the A15 superconductors.

3.2 The axial stress (or strain) effect on the critical current of Nb_3Sn superconductors

As has already been mentioned, Nb_3Sn is a brittle material which in bulk form will fracture at strains of ~0.2 percent. This value however can be comfortably exceeded when Nb_3Sn is in the form of a multifilamentary composite[1]. The stress dependence of the critical current of Nb_3Sn multifilamentary wires varies greatly between samples, as can be seen from Fig. 3.1. In some conductors I_c decreases immediately with strain, whereas in others there is a marked improvement in I_c that strengthens with increased magnetic fields.

An explanation for this behavior lies in the differential thermal contraction between the matrix and the filaments. The precompression in the superconducting filaments, varying greatly between samples depending on the proportions of the constituent materials, causes a

residual degradation in the I_c of the sample. Gradual relief of the precompression with axial tensile stress restores the critical current of the sample toward a maximum. Continued application of tensile stess strains the superconducting filaments further, thereby causing a degradation in I_c. The maxima in Fig. 3.1 correspond to a state at which the filaments are under minimum stress. The controlling parameter is consequently the intrinsic strain on the filaments, rather than the observed overall strain on the wire. Figure 3.2 shows the data of Fig. 3.1 replotted in terms of reduced critical current, I_c/I_{cmax}, and intrinsic strain, $\varepsilon-\varepsilon_{max}$. The apparently very diverse results of Fig. 3.1 may thus be accumulated into a single, unifying curve.

In Nb_3Sn wires, the quantity I_{co}/I_{cmax} is a measure of the residual I_c-degradation of the wires as a result of prestrain, ε_{max}. I_{co} represents the value of the critical current of the wire upon cooldown to 4.2K, with no applied stress or strain. Average values for bronze process Nb_3Sn wires are ε_{max}=0.2-0.3% and I_{co}/I_{cmax}=0.8-0.9 at 12-15T[32].

It was recognized by Ekin[36,37,38,39,40] that the variation of I_c with strain is a secondary effect, the primary one being the reversible strain sensitivity of the upper critical field, B_{c2}. Figure 3.3 shows the effect of axial strain on the upper critical magnetic field of practical A15 superconducting wires. In Fig. 3.3, B_{c2} has been normalized by its maximum (nearly strain-free) value, B_{c2max}. Note that Nb_3Al superconductors are the least susceptible to degradation from uniaxial strain.

It is currently generally accepted that the intrinsic strain, $\varepsilon-\varepsilon_{max}$, derived from one-dimensional considerations, albeit practical, is a widely oversimplified description of the state of the strain, residual or otherwise, in multifilamentary Nb_3Sn wires[31]. The state of strain in a multifilamentary Nb_3Sn wire is three-dimensional, and it is best described in terms of a distortional (or deviatoric) and a hydrostatic (or dilatational) component. The distortional component is the dominant cause of degradation in the superconductivity of a wire, nevertheless the hydrostatic component contributes a nonnegligible influence. Distortional strain is usually represented by the following geometric-average-strain equation, otherwise known as the effective strain[27,28]:

$$\varepsilon_{eff} = \frac{\sqrt{2}}{(1+\nu)} \sqrt{(\varepsilon_r-\varepsilon_\theta)^2 + (\varepsilon_\theta-\varepsilon_z)^2 + (\varepsilon_z-\varepsilon_r)^2} \qquad (3.1)$$

where v is the superconducting material's Poisson's ratio. At zero intrinsic strain when $I_c=I_{cmax}$, the distortional component of strain is at a minimum. It has been shown by X-ray and neutron diffractometry that at this state the tetragonally distorted A15 phase has become approximately cubic.

Already a large database exists for the effect of axial tensile stress and strain on the critical current of A15 superconductors. The same is not true for the transverse stress effect. The severe nature of the latter was recently recognized by Ekin[41,42] and by Specking et al.[32,33]. The transverse stress effect on the critical current of A15 superconductors, all-too-important for tokamak fusion, has since evolved into a major focal point of research in the field of superconductivity.

3.3 The transverse stress effect on the critical current of Nb_3Sn superconductors

Recently it was observed that multifilamentary Nb_3Sn superconductors suffer a large reversible degradation when subjected to uniaxial compressive stress transversely to the conductor axis. Ekin[41,42] has reported that in bronze-process multifilamentary Nb_3Sn and at an applied field of 10T, the magnitude of the transverse stress effect is about seven times larger than the axial stress effect. At 10T and 50MPa he measured a degradation of the I_c of the test-sample of a little less than 10 percent, whereas at 100MPa of nearly 30 percent. At 10T and upon application of 200 MPa of axial stress on an identical wire, he measured a critical current degradation of less than 2 percent.

As with the axial stress effect, the transverse stress effect strengthens with increased magnetic fields, and consequently stems from a reversible degradation of the upper critical field of the superconductor. Ekin[41,42] reported that the intrinsic stress-sensitivity of the upper critical field of bronze-process multifilamentary Nb_3Sn is about ten times greater under transverse stress than under axial stress. It is not obvious why there should exist such a dramatic difference between the transverse and the axial stress effects, however one possible explanation is radial anisotropy in the superconducting reaction layer of a wire, given that the growth pattern in multifilamentary

wires is radial. The answer to this question is pending, nevertheless it is expected to benefit from current metallurgical research.

Despite the severe nature of the transverse stress effect in comparison with the axial stress effect, transverse stresses in a magnet will exist in smaller magnitudes than axial stresses. As was mentioned earlier, the transverse stress on the overall conductor scales with the thickness of the conductor, t, and is consequently smaller than the overall hoop stress which scales with the radius of the winding, R. Nevertheless, preventing degradation of the performance of a magnet from transverse stresses is expected to be a focal point of future conductor design. There will exist upper bounds on the size of the conductors for large-scale, high-field magnet applications, and also significant attention will have to be directed in their internal design. Cable-in-conduit conductors for example, consisting of braided strands, are expected to be particularly susceptible to transverse stress effects in view the fact that there might exist considerable stress concentrations at strand crossover points.

Specking et al.[32,33] have reported that in the NET (Next European Torus) toroidal-field coil study the calculated transverse pressure acting on the conductor reaches values as high as 149MPa in the low field region. Moreover at the Japan Atomic Energy Research Institute (JAERI), the team responsible for the design of FER's (Fusion Experimental Reactor) toroidal coils have estimated transverse stresses as high as 300MPa at the leg of the D-shaped coils by dint of the overturning force. It is not clear what percentage of the transverse stress on the conductors reaches the strands, nevertheless an estimate would be around 50 percent.

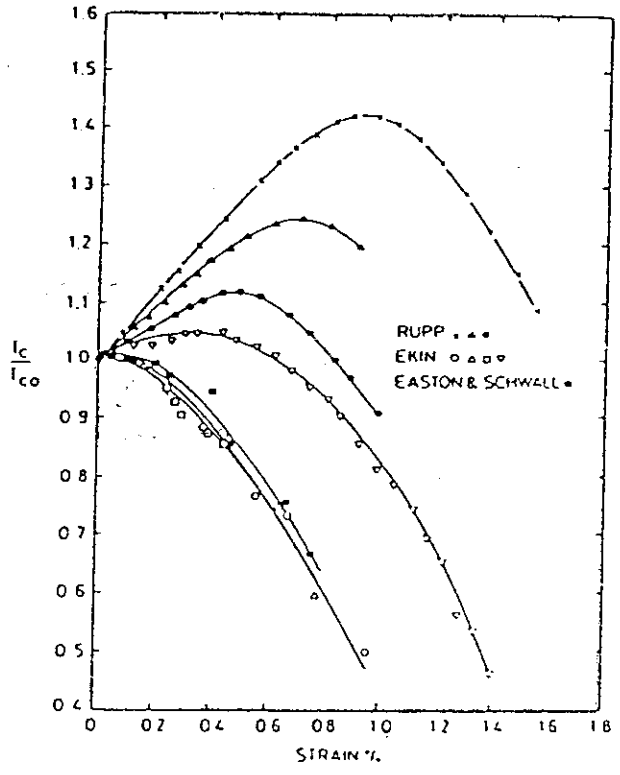

Fig. 3.1 Effect of axial tensile strain on the critical current of various Nb_3Sn composite multifilamentary wires[1,39]

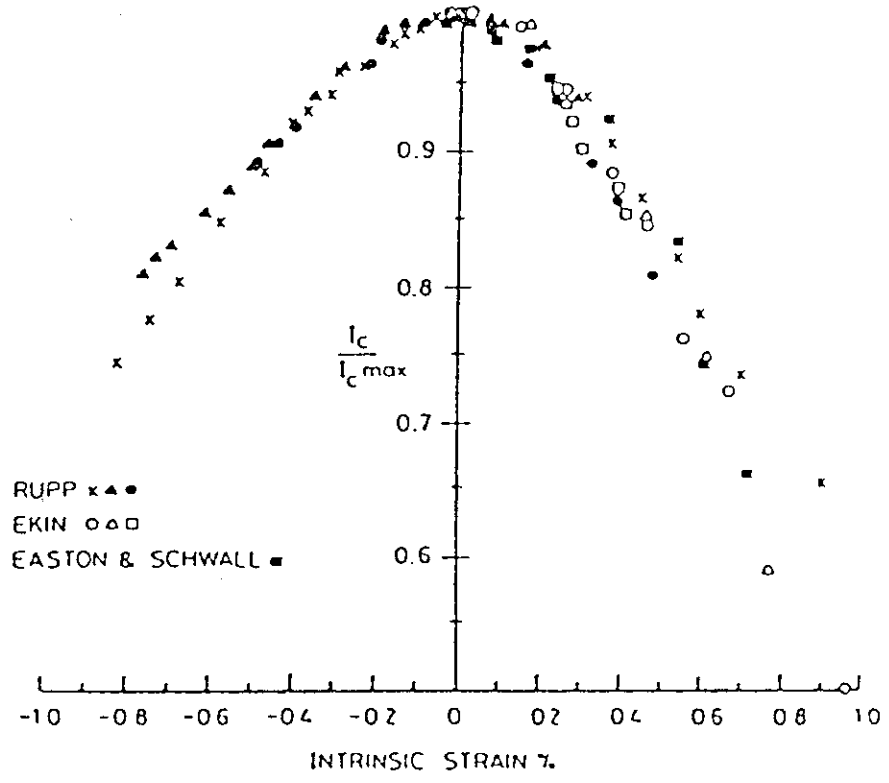

Fig. 3.2 Dependence of the critical current of Nb_3Sn composite multifilamentary wires on the intrinsic strain in the Nb_3Sn filaments[1,39]

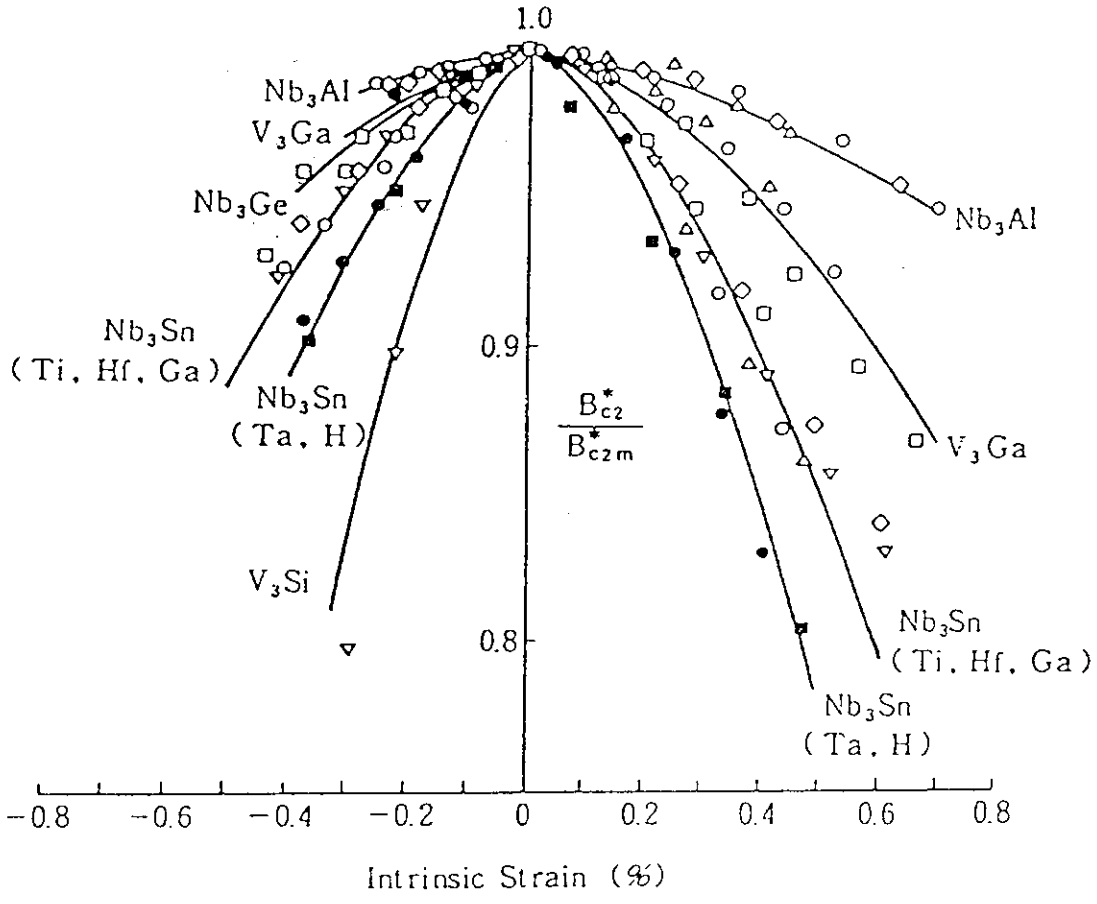

Fig. 3.3 Effect of axial strain on the upper critical field of A15 superconducting wires[40]

4. Apparatus

The experimental arrangement consisted of a 1,000-litter cryostat, a 70mm-bore 15T background magnet, and the transverse compressive stress apparatus. A comprehensive view of the experimental arrangement may be found in Fig. 4.1.

The body of the transverse compressive stress apparatus, designed to be enclosed entirely within the cryostat, consisted of a tubular stainless steel frame housing the transverse load mechanism. The lower part of the tubular construction, terminating at the sample holder and the anvil arrangement for the application of transverse loads, was of 60mm-diameter and could be inserted in the bore of the background magnet. The design was such that the compressed section of the sample would be located at the point of maximum magnetic field. The direction of the transverse load and the magnetic field would both be vertical, perpendicular to the direction of the transport current through the sample.

The transverse load mechanism within the tubular frame consisted of a simple pulling rod arrangement. At the top end, the main pulling rod was connected through a digital load cell to a servo motor. The servo motor could be operated by remote control and could apply with accuracy prescribed loads up to 100kgf. At the lower end, the main pulling rod would split into two smaller, parallel pulling rods at whose ends was attached the bottom half on the anvil arrangement. Activation of the motor would lead to the motion of the latter and thereof to the application of transverse compressive loads.

Figure 4.2 shows two views of the lower part of the transverse compressive stress apparatus. One may thus see the main pulling rod attachment and the two pulling rods linking it to the movable half of the anvil arrangement. The latter consisted of a stainless steel base, a Fiber Reinforced Plastic (FPR) insulator and attachment for the anvil head, and the bottom anvil head, of flat surface and made of stainless steel. Figure 4.2 also shows the FPR sample holder onto which is attached the top, stationary, stainless steel anvil head, as well as the arrangement for current supply. One may thus see the two insulated copper current leads and their respective terminations.

The sample hold was grooved along its length to the precise shape of the U-shaped test samples, such that during experiment the samples would be adequately supported against lateral motion under the action

of the Lorenz force. To the same effect the top anvil head's surface was not flat but had been machined into the shape of a step. The central straight section of the test samples therefore, which for the purposes of transverse compression was to be exposed and could not be inserted into the groove, would be supported unidirectionally against the Lorenz force by the step on the top anvil head. Figure 4.3 shows a cross-sectional view of the sample attachment. As can be seen, a sample could be compressed only along a 10mm section at its center, this length corresponding to the width of the bottom anvil head. At 12mm the top anvil head was slightly wider, to allow for the unimpeded upward motion of the bottom anvil head. As can also be seen from Fig. 4.3, the section of the sample directly above each of its curved knees, in other words the section on each side of the sample extending heyond the sample holder, was soldered onto the current contacts during preparation for experiment.

Several samples were available for experimentation, of the same shape but of different diameters. Different diameter samples required grooves on the sample holder of different clearances. As such, the sample holder was designed to be modular and two different ones were interchanged. One of groove clearance 1mm for samples of diameter less than 1mm, and another of groove clearance 2mm for samples of diameter more than 1mm.

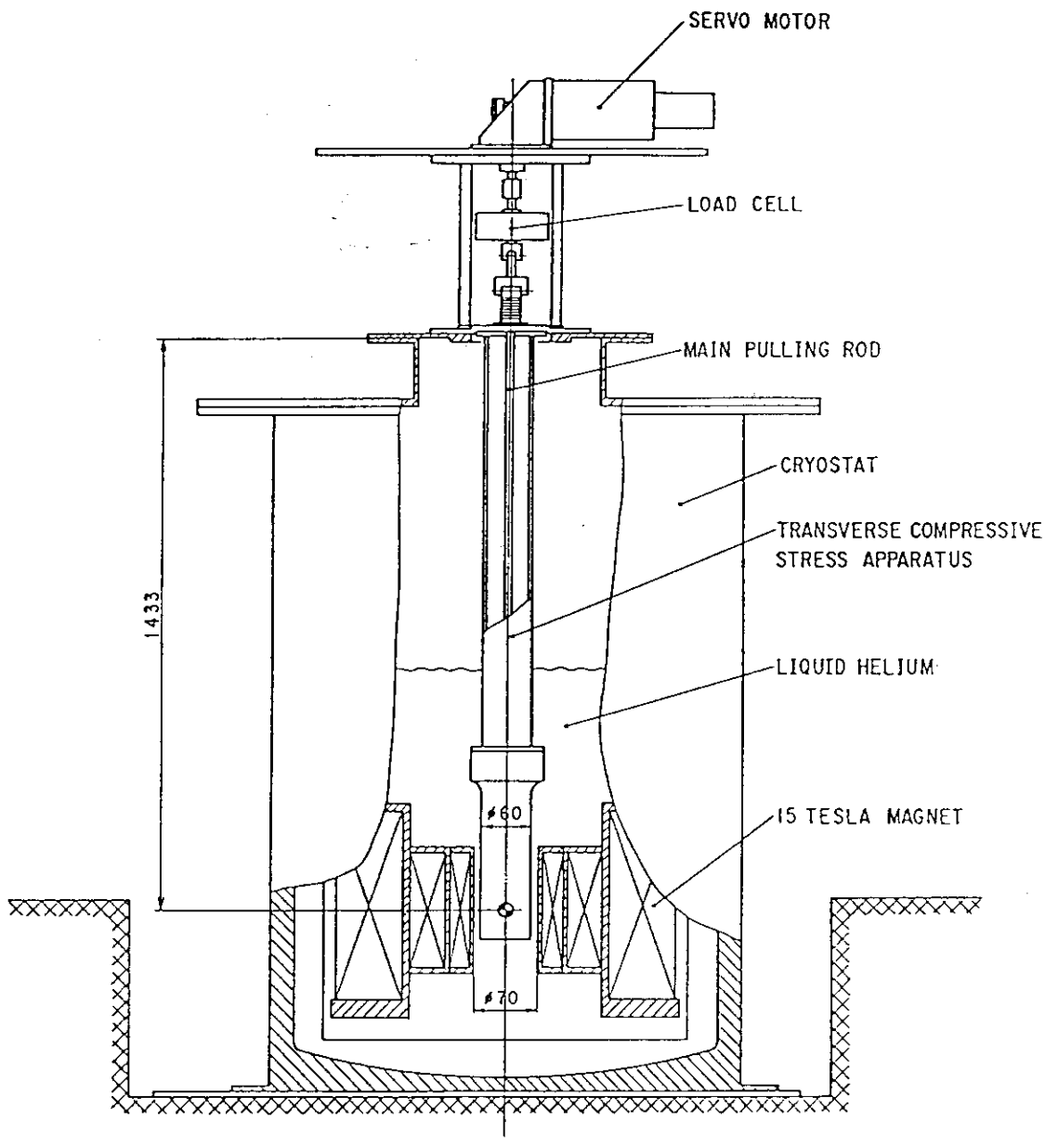

Fig. 4.1 Comprehensive view of the experimental arrangement

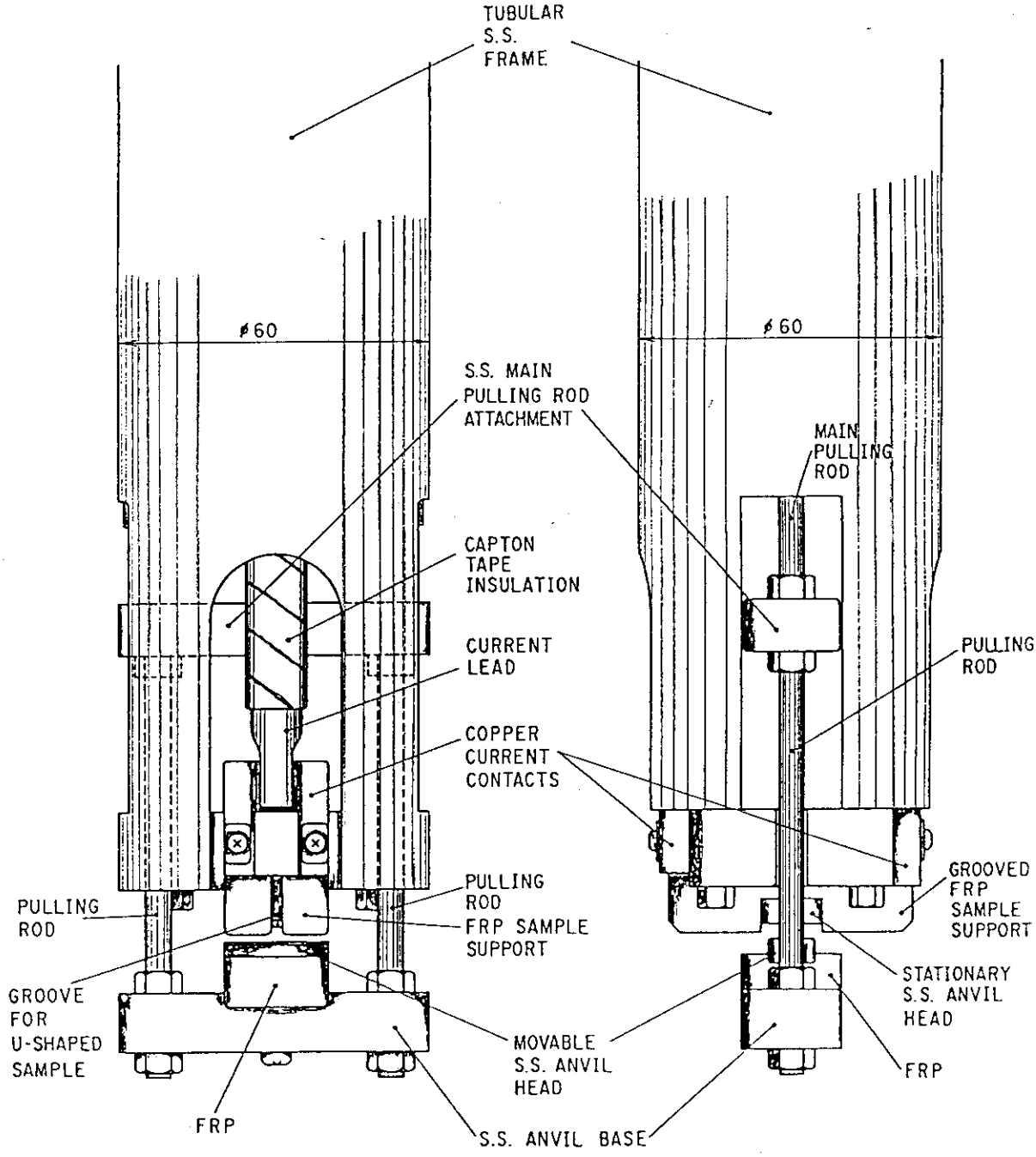

Fig. 4.2 Two views of the transverse compressive stress apparatus

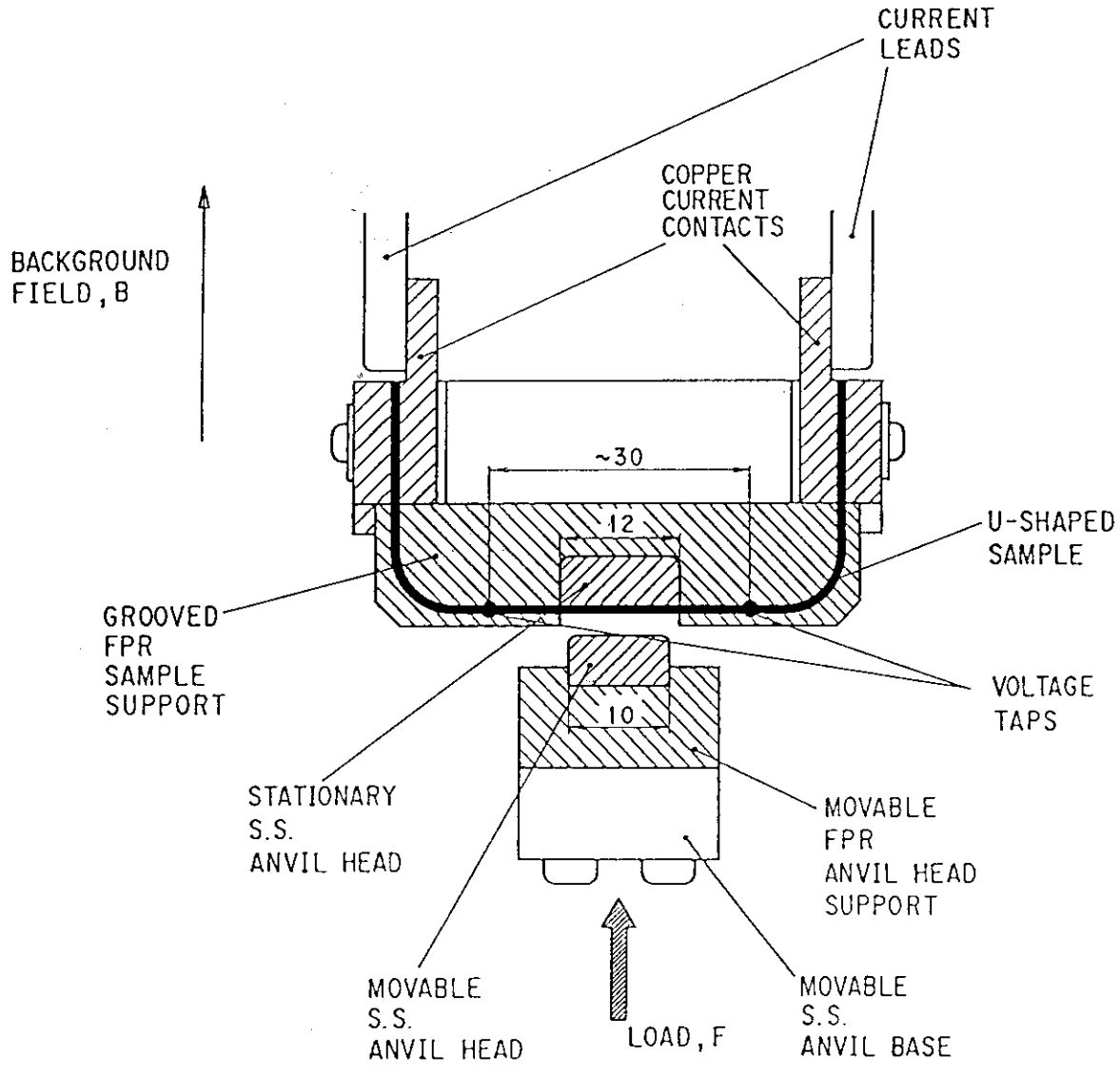

Fig. 4.3 Cross-sectional view of the arrangement for the application of transverse compressive stress

5. Experiment

5.1 Sample installation

Installation of a sample on the transverse compressive stress apparatus was a quick and easy process. First, the movable anvil base would be removed from the apparatus and the appropriate sample holder would be fitted to it. The sample, complete with voltage taps, would be carefully inserted into the groove of the sample holder and then soldered firmly onto the current contacts. The movable anvil base would be attached to the apparatus once again, carefully such that the pressure-surface of the anvil head would be perfectly horizontal for uniform application of transverse compressive stress on the sample. The entire apparatus would then be inserted, or reinserted, into the cryostat.

Two pairs of voltage taps would invariably be soldered onto each sample. One pair would be soldered at the height of the current contacts. The other pair, used to monitor resistivity and thus to measure the critical current of the sample, would be soldered on the horizontal straight section of the sample, typically spanning 30mm in equal halves from its center. Careful attention was always paid on the quality of contact of the voltage taps on the sample. As such, each sample was immersed for a short time in a weak solution of HNO_3, to remove impurities on its surface typically stemming from oxidization of the copper stabilizer. After careful measurements of the new diameter of the sample, usually negligibly smaller than before acid treatment, the voltage taps would be soldered to it.

5.2 Experimental procedure

With the 15T magnet and the transverse stress apparatus in place within the cryostat, cooldown of the system to cryogenic temperatures would be initiated. First the system would be cooled to 77K by liquid nitrogen, then to 4.2K by liquid helium. Throughout the experiment a constant flow of liquid helium would be kept, to compensate for the thermal losses of the system and thus to keep the liquid helium level within the cryostat approximately constant.

Each experiment consisted of measuring the critical current of a sample, under different magnetic fields and levels of transverse compressive stress, using the 10^{-13} Ωm-resistivity criterion. Resistivity versus transport current measurements were made on an XY recorder, Y corresponding to the resistive voltage from the voltage taps, X to the transport current from a 500A/50mV shunt resistor in series with the 500A power supply of the transverse stress apparatus. A typical experiment would first involve measuring the critical current of the sample at zero transverse stress and magnetic fields from 8T to 15T, to establish its J_c vs. B characteristic. The J_c of a sample was calculated for the non-copper section of it. Thereafter transverse compressive stress would be applied in steps of 10 or 20MPa up to the maximum of approximately 200MPa, and critical current measurements would be performed at 12T for every transverse stress level, and also at two additional levels of the magnetic field, typically at 8T and 15T, for every other level.

To establish the J_c vs σ_t behavior of a particular test sample, where σ_t is the applied transverse compressive stress, the digital reading from the load cell, given in units of kgf, was converted into stress by the following formula:

$$\sigma_t = \frac{F_{loadcell}\, g}{L_{compression}\, D_{sample}} \tag{4.1}$$

where $F_{loadcell}$ is the reading in kgf from the load cell, g is the acceleration of gravity, $L_{compression}$ is the length along which transverse compressive stress is applied on the sample, equal to 10mm, and D_{sample} the diameter of the sample. The above formula for computing the applied transverse stress on the sample, though locally incorrect for round samples since the area of contact between the anvill heads and sample increases with increasing loads, is presumed to give a fairly accurate measure of the average state of transverse stress of the superconducting filaments. It is bound to be more accurate for samples containing ample proportions of external stabilizing copper, since thus the transverse load may be uniformly distibuted into the filament region. Under transverse stress, all the components of a filamentary superconductor may be thought of as being in series, experiencing approximately the same stress. Under axial stress however, the components of a filamentary superconductor are loaded in parallel,

therefore the stress is divided proportionately among them.

A problem was unfortunately encountered during experimentation with the controller of the servo motor. Hence the servo motor was substituted by a manual device, which was essentially a mechanical jack system. The advantages of accurate setting and remote control were lost, nevertheless the jack system proved an effective alternative toward the application of transverse compressive stresses.

5.3 Samples

Table 5.1 below presents the essential specifications of all the tested samples, as provided by the manufacturers of the samples. Figure 5.1 presents enlarged views of their cross-sections. The samples experimented upon were two jelly-roll Nb_3Al samples manufactured by Sumitomo Electric Industires, one bronze process Nb_3Sn sample manufactured by Furukawa Electric Industries, and one internally-stabilized bronze process Nb_3Sn sample manufactured by Kobe Steel Ltd. The main focus of the experiments was to establish the transverse stress behavior of jelly-roll Nb_3Al, primarily at 12T but also at other magnetic fields. Also, to compare the transverse stress behavior of jelly-roll Nb_3Al to that of bronze process Nb_3Sn.

Table 5.1 Specifications of test-samples

SAMPLE NUMBER	S1	S2	F1	K4
SUPER-CONDUCTOR	Nb_3Al	Nb_3Al	Ti-ALLOYED Nb_3Sn	Ti-ALLOYED Nb_3Sn
FABRICATION PROCESS	JELLY-ROLL	JELLY-ROLL	BRONZE PROCESS	BRONZE PROCESS w/ INTERNAL Cu STABILIZER
WIRE DIAMETER	1.03mm	0.8mm	1.0mm	1.09mm
FILAMENT DIAMETER	33μm	26μm	3.5μm	4.6μm
NUMBER OF FILAMENTS	240	240	5,940	8,526
TWIST PITCH	∞	∞	11.5mm	35mm
Cu-TO-NONCu RATIO	3.0	3.0	1.86	0.335
BRONZE-TO-CORE RATIO	N/A	N/A	3.4	3.29
HEAT TREATEMENT CONDITIONS	10 HOURS @ 800° C	5 HOURS @ 800° C	120 HOURS @ 650° C	50 HOURS @ 700° C
PREDICTED CRITICAL CURRENT	131 A @ 8T	121A @ 8T	120A @ 12T	303A @ 12T

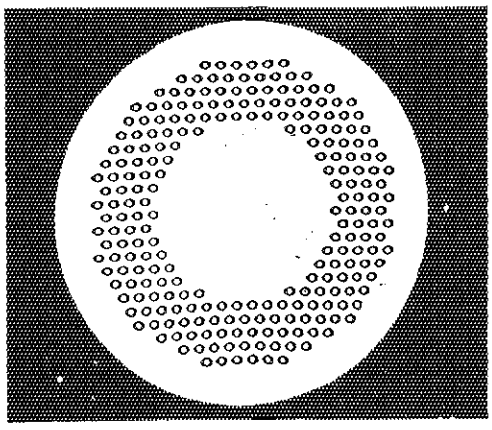

Nb_3Al-S1

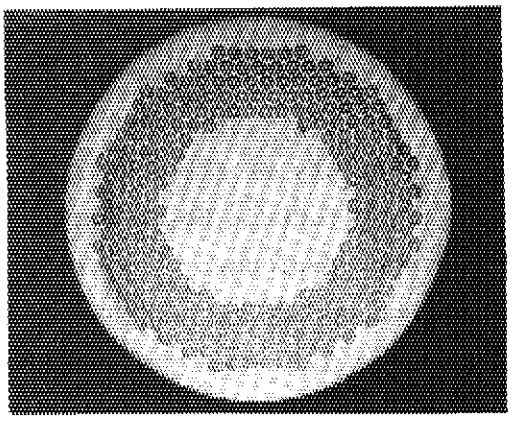

Nb_3Al-S2

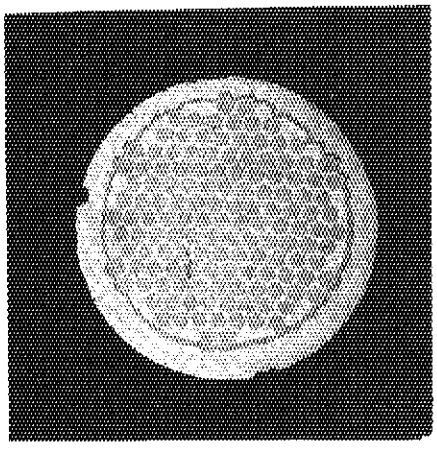

Nb_3Sn-F1

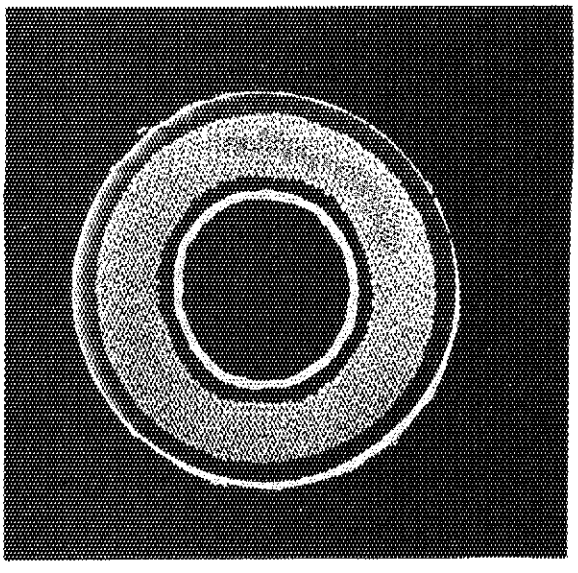

Nb_3Sn-K4

Fig. 5.1 Enlarged cross-sectional views of the test-samples, as provided by the manufacturers.

6. Results and Discussion

6.1 Jelly-roll Nb_3Al-S2

Figure 6.1 shows the measured (non-copper) J_c versus B curve for sample Nb_3Al-S2. At a background field of 12T the measured critical current density of the sample was about 230A/mm^2, an unspectacular value considering current Nb_3Sn wires. It is clear that the wire is in need of further development for improved J_c's at high fields, nevertheless it has the redeeming quality of low transverse stress sensitivity.

Figure 6.2 shows the critical current degradation of the sample with applied transverse stress at the important background field of 12T. I_c is the measured critical current of the sample at various levels of transverse stress at 12T, whereas I_{co} is the measured zero-stress critical current of the sample, also at 12T. It may be seen from Fig. 6.2 that at 12T significant degradation of the I_c starts for transverse stresses above 100MPa. At 100MPa the I_c of the sample is approximately 97 percent of its original zero-stress value, and degrades to a respectable 69 percent at around 200MPa.

Figure 6.3 shows the I_c-degradation of the sample with transverse stress at a background field of 15T, whereas Fig. 6.4 shows the I_c-degradation at 8T. As in the 12T case, significant degradation starts for transverse stresses above 100MPa, where I_c/I_{co} is about 95 percent at 15T and about 97 percent at 8T. Around 200Mpa, I_c/I_{co} is slightly above 61 percent at 15T, and approximately 76 percent at 8T. Overall, the I_c of Nb_3Al-S2 exhibits higher sensitivity to transverse stress at 15T than at 12T, and smaller sensitivity at 8T than at 12T. The same behavior has been reported by researchers for Nb_3Sn wires, nevertheless in the case of Nb_3Al-S2 the difference is hardly noticeable below 100MPa and only very small above 100MPa.

For all three magnetic fields the stress was released from the maximum attained value of about 200MPa to zero. The arrow in Fig. 6.2, 6.3, and 6.4, signifying this stress release, points to the residual I_c-degradation. It may be seen from these figures that upon release of the stress the I_c of the sample recovered only slightly. The reason may be attributed to irreversible plastic deformation of the stabilizing copper surrounding in ample quantities the Nb_3Al filaments. After experiment, the diameter of the sample was flatter by ~8.5 percent in

the direction of compression, and wider by ~7 percent transversely to the direction of compression.

Figure 6.5 combines the data from Fig. 6.2, 6.3, and 6.4 to a cumulative graph displaying the field dependence of the I_c-degradation of Nb_3Al-S2 with transverse compressive stress. Table 6.1 summarizes significant I_c-degradation values at the corresponding transverse stress and magnetic field conditions.

Figure 6.5 displays a rather curious phenomenon. The normalized critical current of Nb_3Al-S2 is slightly enhanced, to a constant value, for transverse stresses between 0 and 100MPa. This effect is most pronounced at 15T, less so at 12T, and is nonexistent at 8T. The phenomenon is unexpected because this enhancement may not be attributed to changes in the strain-state of the compressed section of the wire. The voltage taps, spaced at about 10mm to the left and to the right of the compressed section, could not possibly detect a local enhancement but only a global one, the critical current of a wire being a weak-link problem. A possible explanation for this phenomennon is that the imperfect support of the sample by the sample holder, and also possible alterations in the original setting of it from thermal contraction during cooldown, allow for a certain deformation of the sample upon transverse compression. This deformation may help remove residual precompressions in the Nb_3Al filaments, as is the case for Nb_3Sn wires stressed axially, an effect which strengthens likewise with increased magnetic fields.

6.2 Jelly-roll Nb_3Al-S1

Figure 6.6 shows the measured J_c versus B curve for sample Nb_3Al-S1, alongside that of sample Nb_3Al-S2. The former reflects measurements up to 12T only, because of a problem in the background magnet. At 12T the measured J_c of Nb_3Al-S1 was about 215A/mm^2, slightly inferior to that of the smaller-diameter Nb_3Al-S2. The differences in J_c between the two samples are quite small, given that the two samples are very similar to each other. Nevetheless the differences in J_c are rather more pronounced at lower fields. The reason for these differences may be attributed to the heat treatment conditions (Table 5.1).

Figure 6.7 shows the critical current degradation of sample Nb_3Al-S1

with transverse stress at a background field of 12T. It also shows the recovered I_c/I_{co} of the sample upon release at each level of applied transverse stress. (After experiment, the diameter of the sample was flatter by ~9.5 percent in the direction of compression, and wider by ~6 percent transversely to the direction of compression.) Note once again the curious slight enhancement of the critical current of the sample for transverse stresses of up to 100MPa. It is possibly a variant manifestation of the enhancement phenomenon exhibited by Nb_3Al-S2. One may see from Fig. 6.7 that significant I_c-degradation occurs for transverse stresses above 100MPa, as was the case for sample Nb_3Al-S2. In the vicinity of 100MPa I_c/I_{co} is about 97 percent, whereas in the vicinity of 200MPa it is approximately 58 percent. The latter value compares unfavorably with the equivalent one from sample Nb_3Al-S2, which is about 69 percent.

Figure 6.8 compares the I_c/I_{co} versus σ_t curves of the two samples at a background magnetic field of 12T. Table 6.2 compares the performance of the two samples at 12T and at the key transverse stress values of approximately 100, 160, and 200MPa. The I_c/I_{co} of Nb_3Sl-Sl degrades more sharply for transverse stresses above 100MPa than that of sample Nb_3Al-S2. The curves for the two samples seem to diverge from each other for stresses higher than 120MPa. This is rather unexpected, considering that there are only small differences between the two samples. An explanation for this may be that the formula for estimating stress, in other words that of dividing the applied load by an "effective" area of compression, is incorrect for high loads. At high loads the deformation of the copper surrounding the superconducting filaments is large, so it is possible that non-easily-accountable nonuniformities in the stress distribution within the wires occur. Other explanations could be discontinuities at the edges of the compressed section of the wires, and also heat treatment-induced differences in the radial crystallography of the superconducting section of each wire.

6.3 Bronze process Nb_3Sn-Fl

Figure 6.9 shows the measured J_c versus B curve for sample Nb_3Sn-Fl, against the J_c versus B curve of sample Nb_3Al-S2. It is clear from Fig.

6.9 that Nb_3Sn-F1 has better J_c versus B characteristics than Nb_3Al-S2, especially at high fields. At 8T the J_c of Nb_3Sn-F1 is about 905A/mm^2, about 10 percent higher than that of Nb_3Al-S2 at the same field (~820 A/mm^2). At 12T however, the J_c of the former is about 406A/mm^2, ~45 percent higher than that of the latter at the same field (~230 A/mm^2).

The high J_c at high fields of current Nb_3Sn wires have established them as the dominant conductors for high-field applications. Their main disadvantage is excessive sensitivity to stress, especially to transverse compressive stress. Sample Nb_3Sn-F1 is Ti-alloyed however, and should exhibit lower sensitivity to transverse stress than regular binary Nb_3Sn wires fabricated by the bronze process. As is well-known with regard to the axial stress effect, ternary additions to the superconduting compound, for example Ta or Ti, have the effect of reducing the degradability of the wire's critical properties by stress and strain.

Figure 6.10 shows the critical current degradation of sample Nb_3Sn-F1 with applied transverse stress at a background field of 12T. Degradation starts immediately upon the application of transverse stress. The degradation is rather subdued until about 60MPa, I_c/I_{co} being better than 90 percent at this level, however above 60MPa the it becomes dramatic. In the vicinity of 100MPa I_c/I_{co} is about 75 percent (97 percent for Nb_3Al-S2), whereas in the vicinity of 150-160MPa I_c/I_{co} is impressively low at approximately 35 percent (about 81 percent for Nb_3Al-S2). Release of the maximum applied transverse stress restores the I_c of the sample to about 65 percent of the original zero-stress value. Plastic deformation of the stabilizing copper imparts residual stresses to the bronze/Nb_3Sn core of the wire. Nb_3Sn-F1 does not exhibit the excessive irreversibility of Nb_3Al-S2, since it contains a smaller proportion of copper (the copper ratio is 1.86 for Nb_3Sn-F1, as opposed to 3.0 for Nb_3Al-S2). After experiment, the diameter of the sample was flatter by ~4.5 percent in the direction of compression, and wider by ~3.2 transversely to the direction of compression.

Filament breakage is also a possible cause for the residual degradation, albeit a less likely one. It may be supported by observing in Fig. 6.10 the abrupt drop in I_c of the sample immediately upon the application of transverse stress. Imperfect fitting of the sample in the sample holder, resulting in dimensional mismatches, may be the cause of local damage as the sample is forced to conform to the anvil surfaces upon application of transverse stress.

As shown in Fig. 6.11, the I_c-degradation of Nb_3Sn-F1 is significantly more dramatic at 15T than at 12T. Degradation starts immedicately and steeps down sharply for stresses above only 40MPa. At 100MPa I_c/I_{co} is very low at approximately 52 percent, whereas at around 160MPa it is strikingly low at approximately 10 percent. Conversely, as shown in Fig. 6.12, the I_c-degradation of Nb_3Sn-F1 is less dramatic at 8T than at 12T, I_c/I_{co} being around 88 percent in the vicinity of 100MPa, and approximately 61 percent at around 160MPa. The I_c of the sample recovers to about 80 percent of the zero-stress value at 8T, as contrasted with 65 percent at 12T. An unexpected quench in the background magnet prevented us from taking release data at 15T. Figure 6.13 combines Fig. 6.10, 6.11, and 6.12 to a cumulative graph displaying the field dependence of the I_c-degradation of sample Nb_3Sn-F1 with transverse stress.

The vast intrinsic superiority of Nb_3Al-S2 over Nb_3Sn-F1 with regard to transverse compressive stress is clear, despite the much larger copper-ratio of the former in comparison with the latter (3.0 versus 1.86). At the field of interest of 12T, the I_c of Nb_3Al degrades little up to 100MPa, whereas the I_c of Nb_3Sn degrades by as much as 25 percent at 100MPa. For higher levels of transverse stress Nb_3Sn exhibits degradations as much as a factor of ~3-4 higher than Nb_3Al-S2. Figure 6.14 juxtaposes the normalized critical current versus transverse stress characteristics of the two samples at 12T, whereas Fig. 6.15 and 6.16 at 15T and 8T, respectively. Table 6.3 compares the performance of sample Nb_3Sn-F1 and Nb_3Al-S2 at 8, 12, and 15T and at several key values of applied transverse stress.

6.4 Internally stabilized bronze process Nb_3Sn-K4

Figure 6.17 shows the measured J_c versus B characteristics of sample Nb_3Sn-K4, alongside the J_c versus B curve of sample Nb_3Sn-F1. Again, the former curve reflects measurements of up to 13T only, due to a problem in the background magnet. Also, in the absence of an available high-ampere power supply, the minimum background field for I_c measurements was limited to 10T.

At 12T the J_c of Nb_3Sn-K4 was around 380A/mm^2, a little less than that of Nb_3Sn-F1 at the same field (406A/mm^2). We may see from Fig.

6.17 that the J_c versus B characteristics of the two samples are similar, given that the two samples have very similar composition. The internally-stabilized configuration, the differences in the copper-ratio (0.335 for Nb_3Sn-K4 versus 1.86 for Nb_3Sn-F1), and the different heat treatment conditions (Table 5.1), might be contributing to the slight differences in the J_c versus B behavior of the two samples.

Figure 6.18 shows the critical current degradation of sample Nb_3Sn-K4 with transverse stress at a background field of 12T. It is interesting that, in contrast to the other samples discussed so far at 12T, the I_c/I_{co} versus σ_t curve does not possess a relatively flat section at low transverse stresses, but rather it steeps drastically downward from the beginning. At 100MPa there is significant I_c-degradation, I_c/I_{co} being approximately 55 percent. At 120MPa I_c/I_{co} is about 36 percent, whereas upon release of the latter stress the I_c recovers to about 65 percent of its original zero-stress value. After experiment, the diameter of the sample was flatter by ~2.5 percent in the direction of compression, and wider by ~1.5 percent transversely to the direction of compression.

The rather excessive sensitivity to stress exhibited by this sample must stem from the fact that the copper stabilizer is located at the core of the wire as opposed to externally in the form of a jacket. Transverse stress is consequently applied directly on the bronze that constitutes the external surface of the wire. There is no damping of the stress by an intervening soft layer of copper, and therefore the possibility of an inhomogeneous stress distribution in the superconducting section of the wire is high. The superconducting filaments closer to the surface must be stressed disproportionally to those further away from it, which is not necessarily the case for externally stabilized wires such as sample Nb_3Sn-F1.

At 12T, the I_c of sample Nb_3Sn-K4 drops by almost 10 percent merely upon the application of transverse stress. This phenomenon must come from irreversible damage of the sample, such as filament breakage, as was possibly the case for Nb_3Sn-F1. We are not in a position to explain why this irreversible damage is almost double for Nb_3Sn-K4 than for Nb_3Sn-F1, since we may not preclude the possibility that the former sample was set in the sample holder less deftly than the latter. Nevertheless, breakage of superconducting filaments located close to the surface of sample Nb_3Sn-K4 is quite likely, as a result of the harsh

contact between the external bronze of the sample and the stainless steel anvil heads.

As can be seen from Fig. 6.19 and 6.20, I_c/I_{co} versus σ_t curves at 13T and 10T respectively, sample Nb_3Sn-K4 exhibits the same kind of field dependence as the other samples. Its critical current is more sensitive at higher fields than at lower fields, once again an observation that gives credence to the fact the I_c-degradation in A15 superconductors stems from a reversible degradation of their upper critical magnetic field. Thus, for a transverse stress of 100MPa I_c/I_{co} is approximately 44 percent at 13T, and approximately 64 percent at 10T. The residual I_c/I_{co} of the sample upon release of the maximum applied transverse stress scales similarly for the different fields, being around 65 percent at 13T and around 82 percent at 10T. The same holds true for the initial seemingly irreversible drop of the I_c of the sample, the drop in other words that occurs simultaneously with the application of transverse stress. Figure 6.21 combines Fig. 6.18, 6.19, and 6.20 into a cumulative graph showing the field dependence of the I_c-degradation of sample Nb_3Sn-K4 with applied transverse compressive stress.

Figure 6.22 compares the sensitivity to transverse stresses of the I_c of both Nb_3Sn samples at 12T. Table 6.4 summarizes significant I_c-degradation values at 12T and at several key values of the applied transverse stress. It is evident that Nb_3Sn-F1 is a superior wire with respect to transverse compressive stress. In the vicinity of 100MPa, I_c/I_{co} is 20 percent higher for Nb_3Sn-F1 than for Nb_3Sn-K4. Nevertheless, this superiority must stem from the more favorable externally-stabilized configuration which, as has already been mentioned, is a more advantageous configuration for most applications.

Figure 6.23 compares all tested samples at a background magnetic field of 12T. The Nb_3Al samples are the least sensitive to transverse compressive stresses, especially for values below 100MPa. The reason is most probably intrinsic to the Nb_3Al phase, traceable in other words to the crystallography of the superconductor.

Table 6.1 I_c-degradation values for sample Nb_3Al-S2

TRANSVERSE STRESS(MPa)	MAGNETIC FIELD (T)	ZERO-STRESS CRITICAL CURRENT, I_{co} (A)	CRITICAL CURRENT DENSITY, J_{co} (A/mm^2)	NORMALIZED CRITICAL CURRENT, I_c/I_{co}
~100	8	103	819.41	~97%
~200	"	"	"	~76%
~100	12	29	230.71	~97%
~200	"	"	"	~69%
~100	15	8	63.64	~95%
~200	"	"	"	~61%

Table 6.2 Comparison of I_c-degradation values for samples Nb_3Al-S2 and Nb_3Al-S1

SAMPLE	Transverse STRESS (MPa)	MAGNETIC FIELD (T)	Zero-stress CRITICAL CURRENT, I_{co} (A)	CRITICAL CURRENT DENSITY, J_{co} (A/mm^2)	Normalized CRITICAL CURRENT, I_c/I_{co}
	~100	12	29	230.71	~97%
Nb_3Al-S2	~160				~81%
	~200				~69%
	~100	12	44.75	214.83	~97%
Nb_3Al-S1	~160				~72%
	~200				~58%

Table 6.3 Comparison of I_c-degradation values for samples Nb_3Al-S2 and Nb_3Sn-F1

SAMPLE	Transverse STRESS (MPa)	MAGNETIC FIELD (T)	Zero-stress CRITICAL CURRENT, I_{co} (A)	CRITICAL CURRENT DENSITY, J_{co}(A/mm^2)	Normalized CRITICAL CURRENT, $I_c/I_{c\,0}$
Nb3Al-S2	~60	8	103	819.41	~100%
	~100				~97%
	~140				~89%
	~60	12	29	230.71	~99%
	~100				~97%
	~160				~81%
	~60	15	8	63.64	~105%
	~100				~95%
	~140				~80%
Nb3Sn-F1	~60	8	248.75	905.86	~95%
	~100				~88%
	~160				~61%
	~60	12	111.5	406.05	~92%
	~100				~75%
	~150				~35.5%
	~60	15	47	171.16	~82%
	~100				~52.5%
	~160				~10.7%

Table 6.4 Comparison of I_c-degradation values for samples Nb_3Sn-F1 and Nb_3Sn-K4

SAMPLE	Transverse STRESS (MPa)	MAGNETIC FIELD (T)	Zero-stress CRITICAL CURRENT, I_{co} (A)	CRITICAL CURRENT DENSITY, J_{co} (A/mm^2)	Normalized CRITICAL CURRENT, Ic/Ico
Nb3Sn-F1	~60	12	111.5	406.05	~92%
	~100				~75%
	~120				~60%
Nb3Sn-K4	~60	12	265	379.11	~75%
	~100				~55%
	~120				~36%

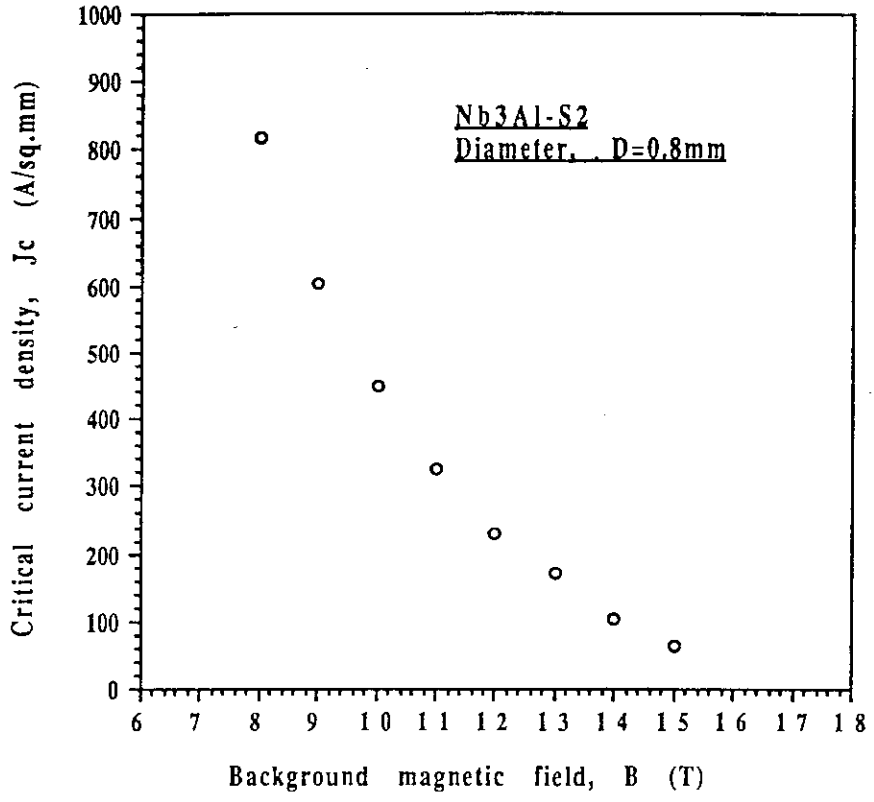

Fig. 6.1 J_C versus B curve for sample Nb_3Al-S2

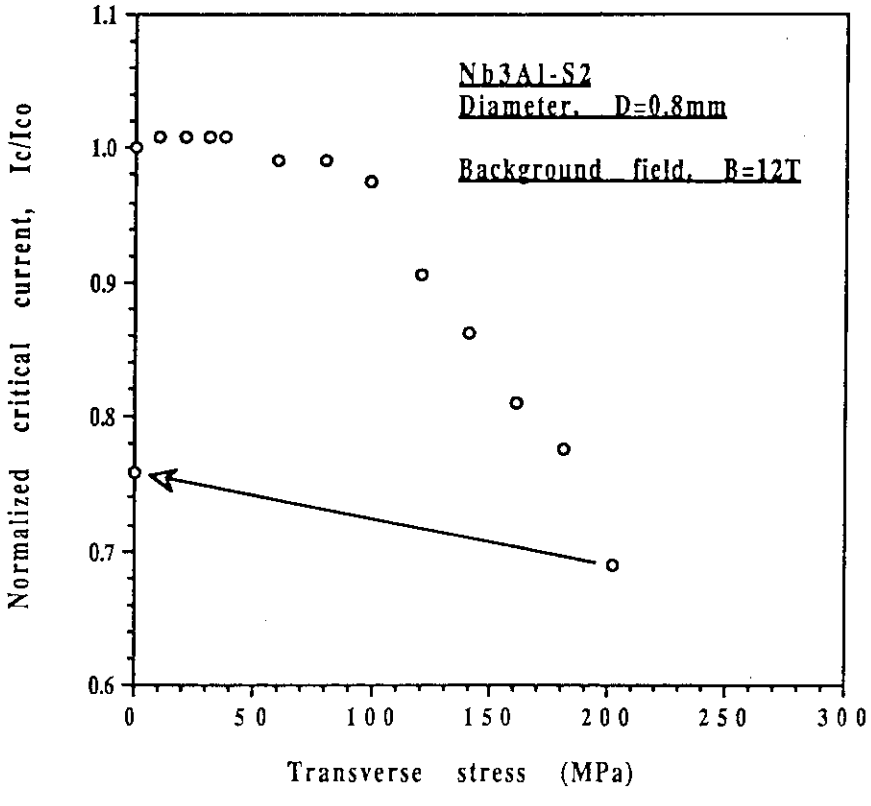

Fig. 6.2 I_C/I_{CO} versus σ_t at 12T for sample Nb_3Al-S2

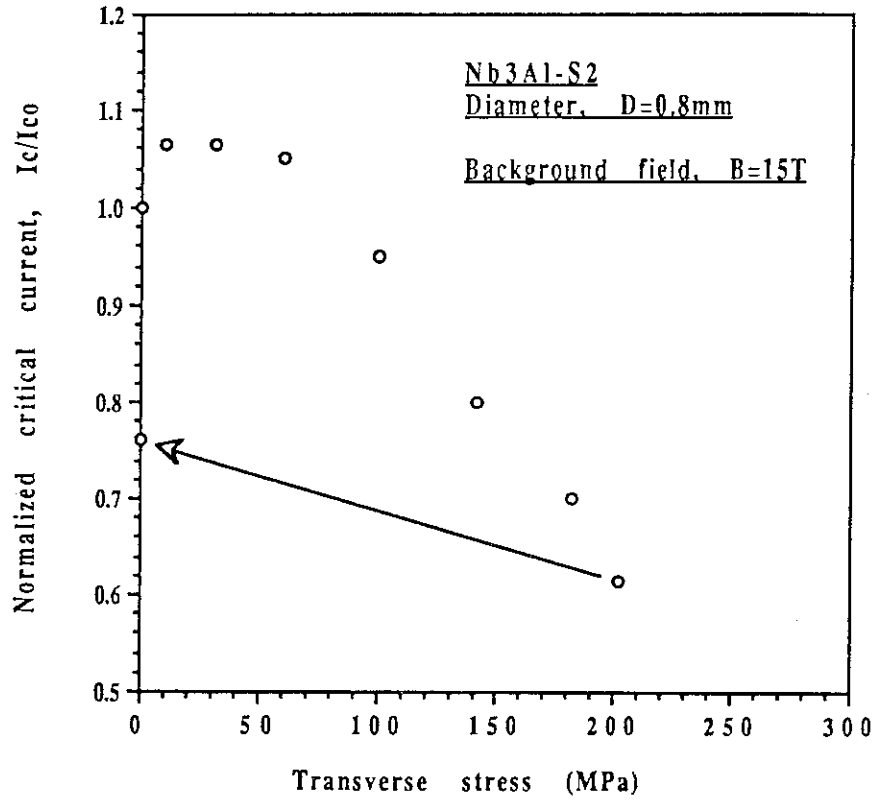

Fig. 6.3 I_c/I_{co} versus σ_t at 15T for sample Nb_3Al-S2

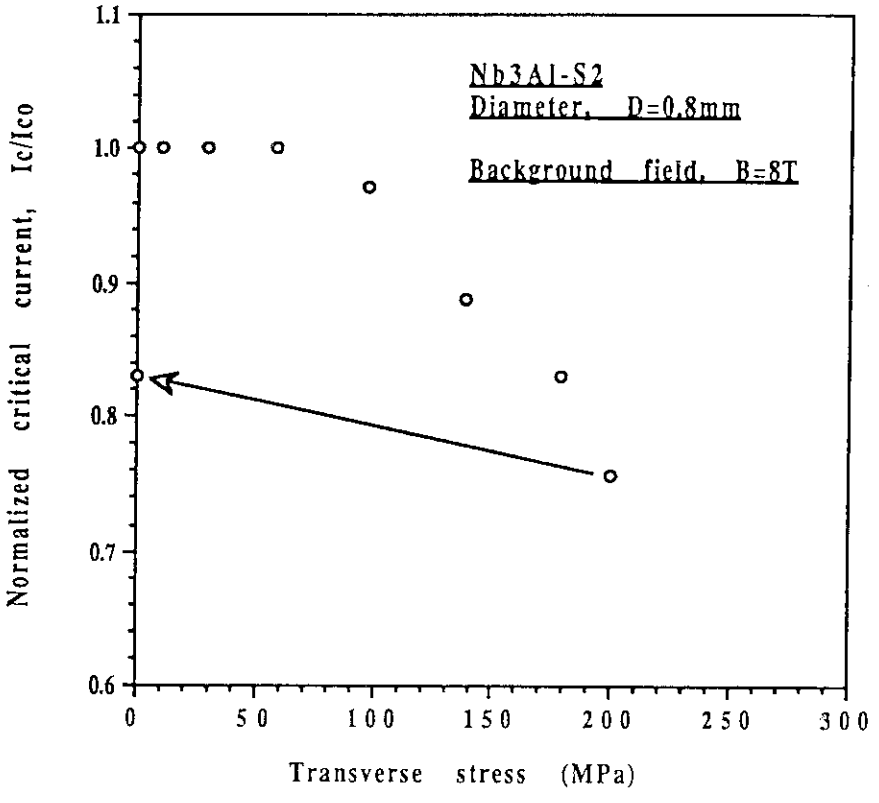

Fig. 6.4 I_c/I_{co} versus σ_t at 8T for sample Nb_3Al-S2

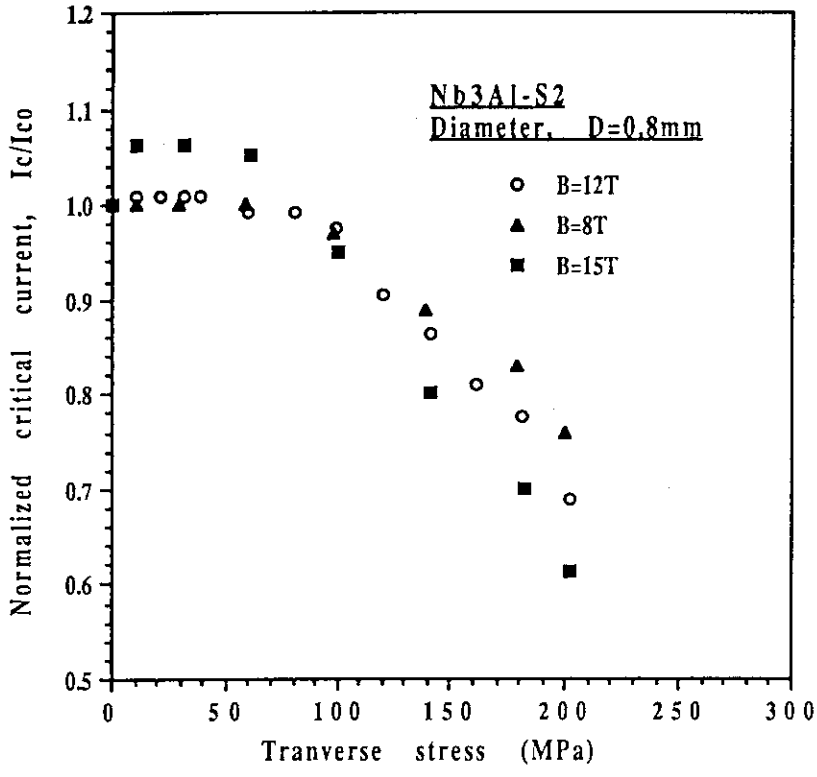

Fig. 6.5 I_c/I_{co} versus σ_t at different fields for sample Nb_3Al-S2

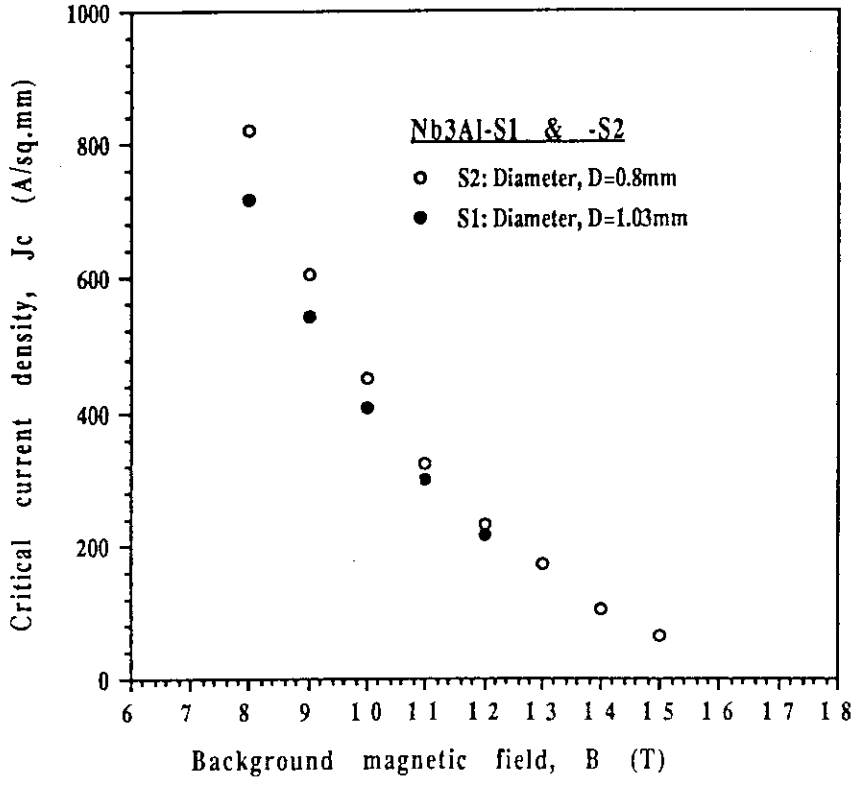

Fig. 6.6 J_c versus B for samples Nb_3Al-S1 and Nb_3Al-S2

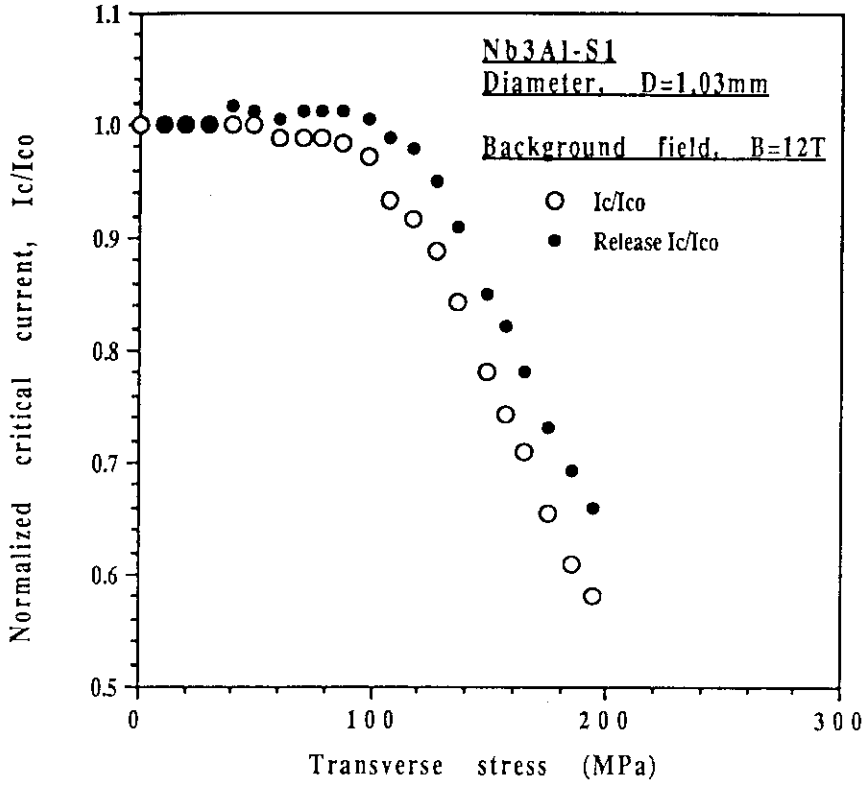

Fig. 6.7 I_c/I_{co} versus σ_t at 12T for sample Nb_3Al-S1

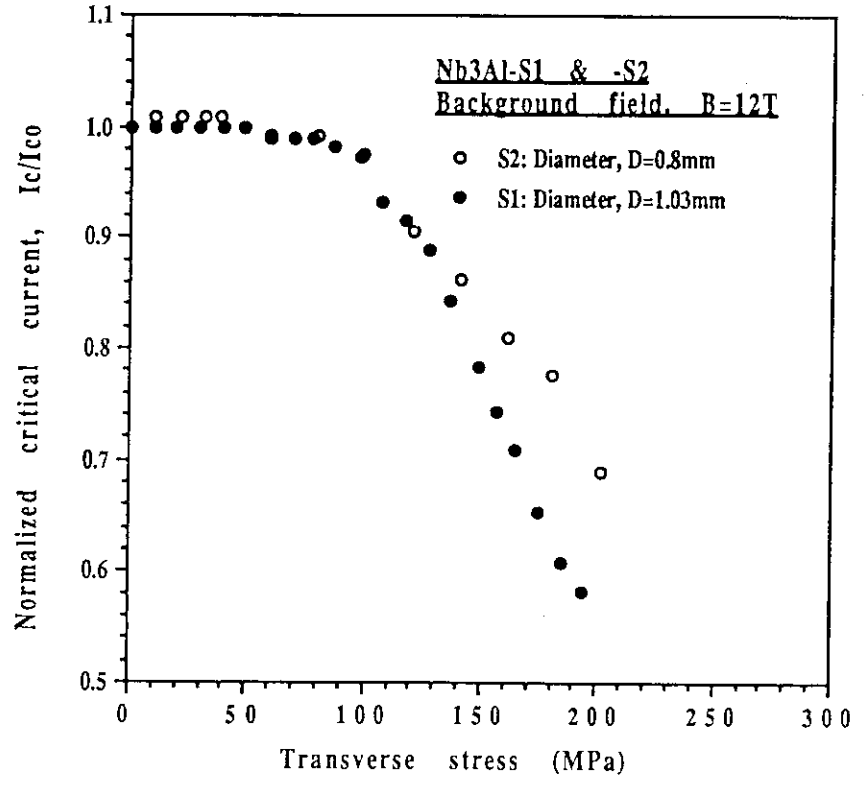

Fig. 6.8 I_c/I_{co} versus σ_t for samples Nb_3Al-S1 and Nb_3Al-S2

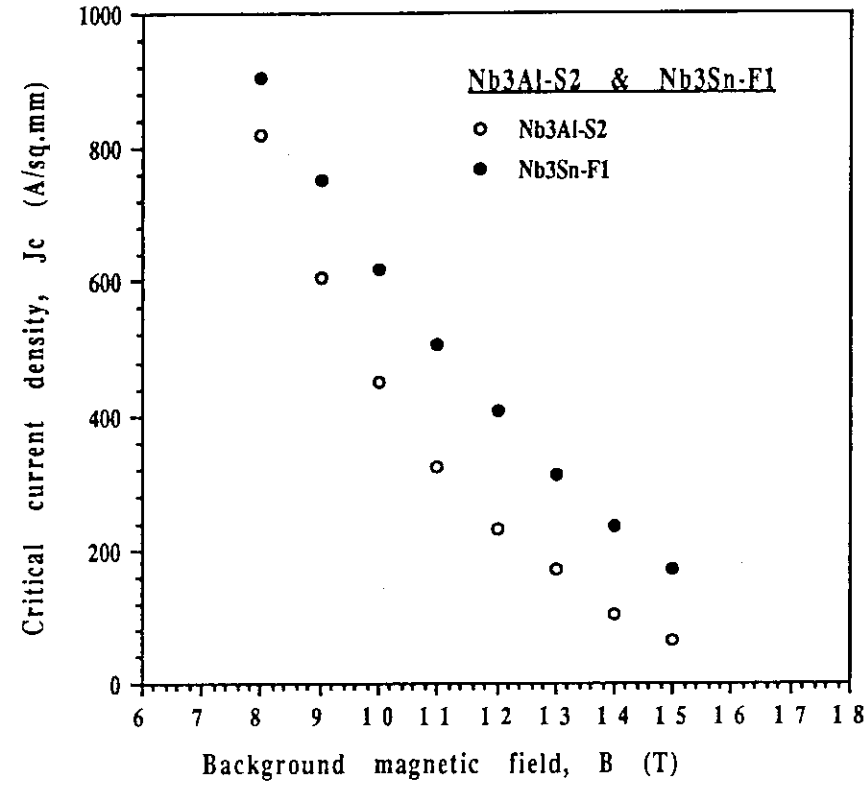

Fig. 6.9 J_c versus B for samples Nb_3Sn-F1 and Nb_3Al-S2

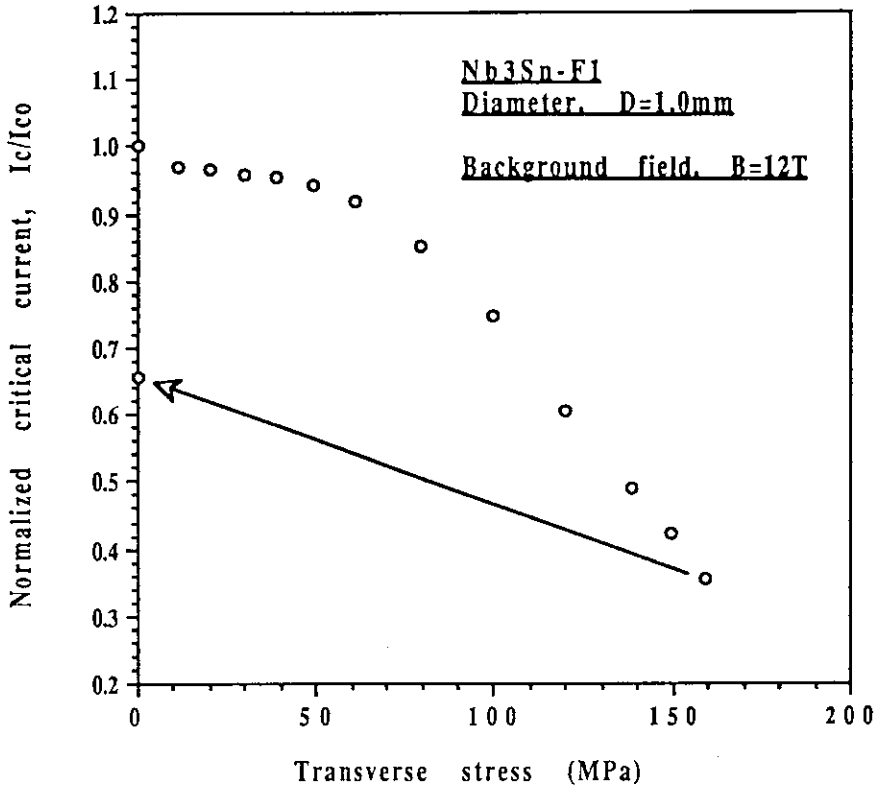

Fig. 6.10 I_c/I_{co} versus σ_t at 12T for sample Nb_3Sn-F1

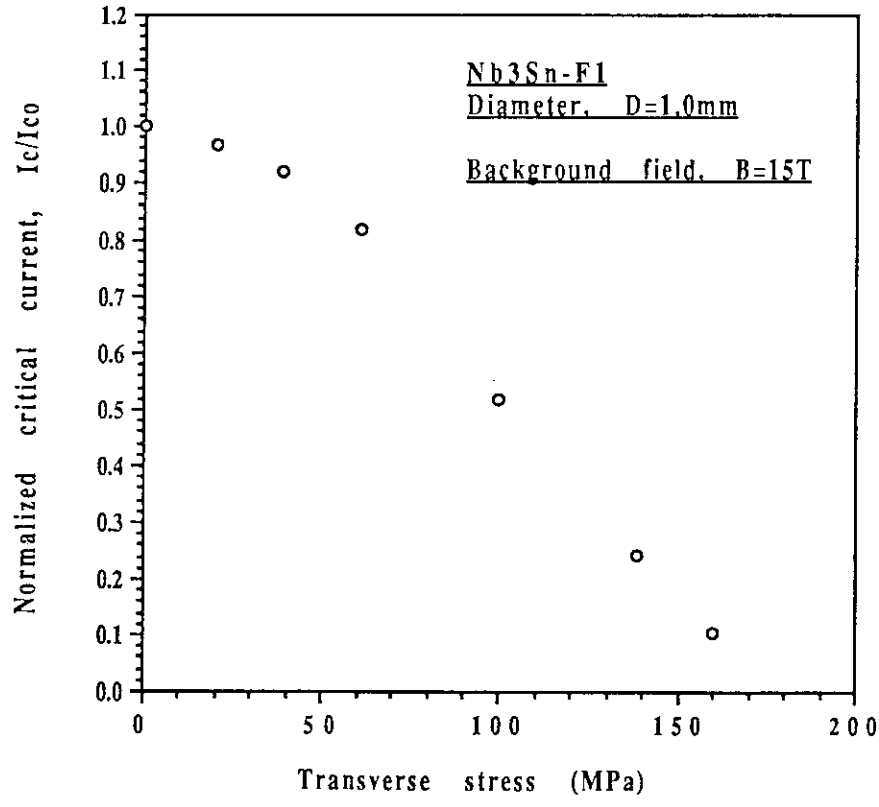

Fig. 6.11 I_c/I_{co} versus σ_t at 15T for sample Nb_3Sn-F1

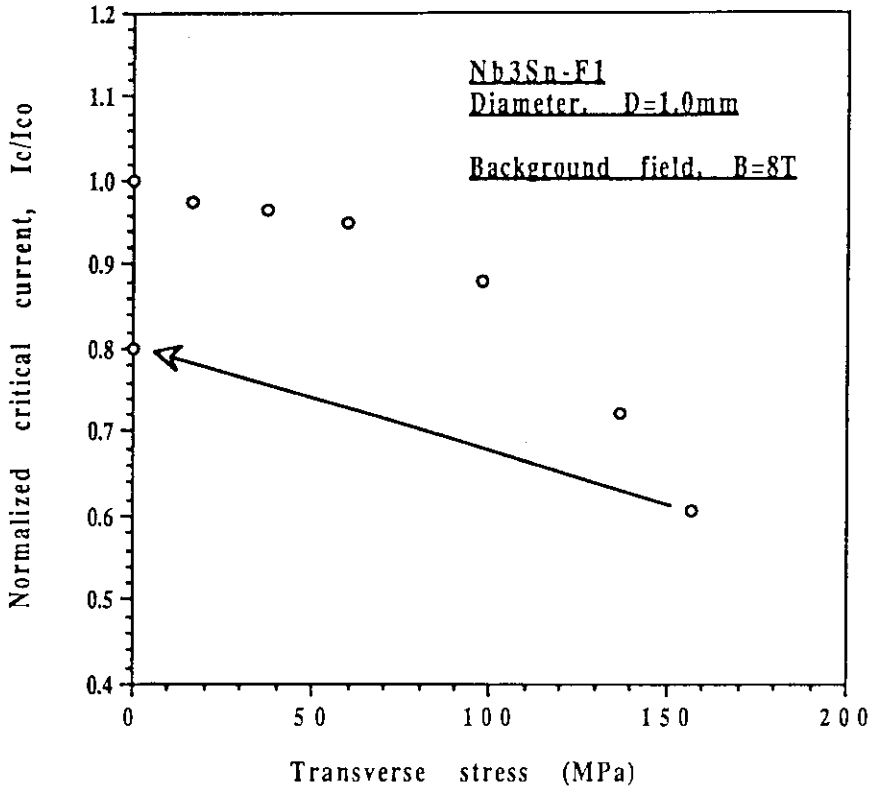

Fig. 6.12 I_c/I_{co} versus σ_t at 8T for sample Nb_3Sn-F1

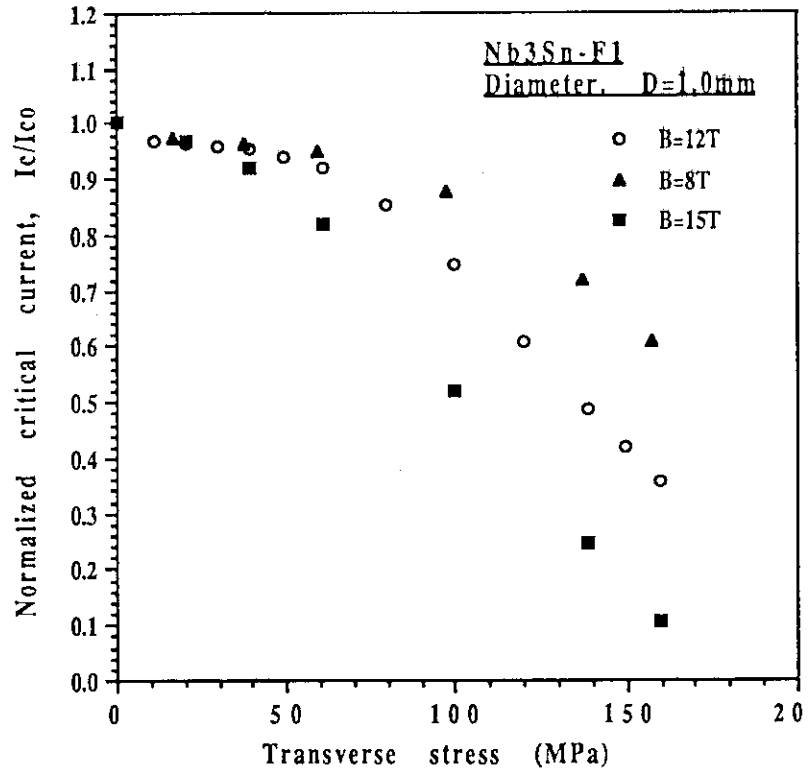

Fig. 6.13 I_c/I_{co} versus σ_t at different fields for sample Nb_3Sn-F1

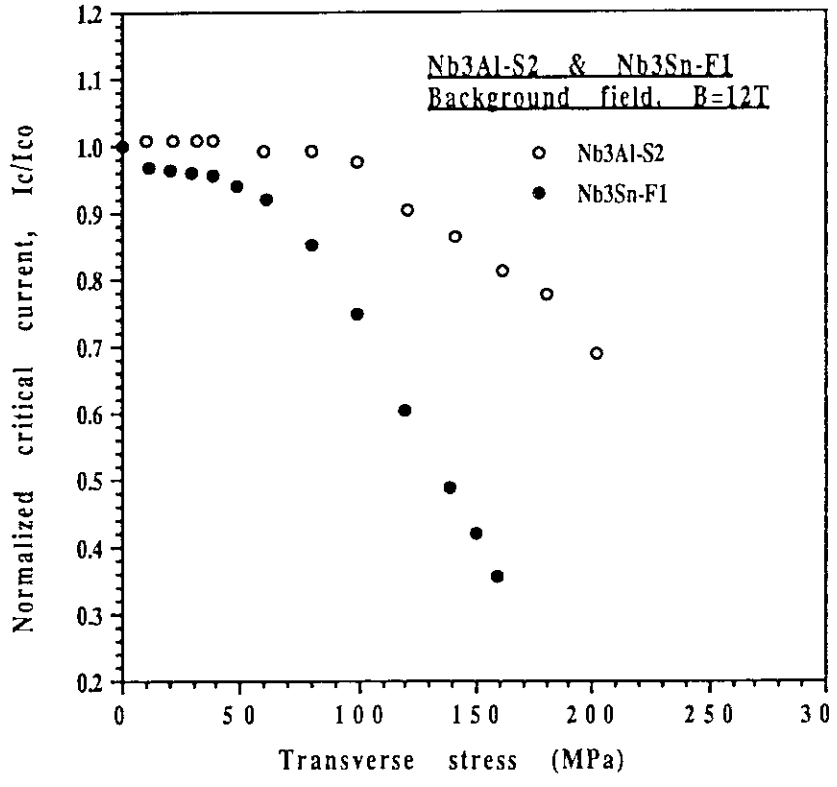

Fig. 6.14 I_c/I_{co} versus σ_t at 12T for samples Nb_3Sn-F1 and Nb_3Al-S2

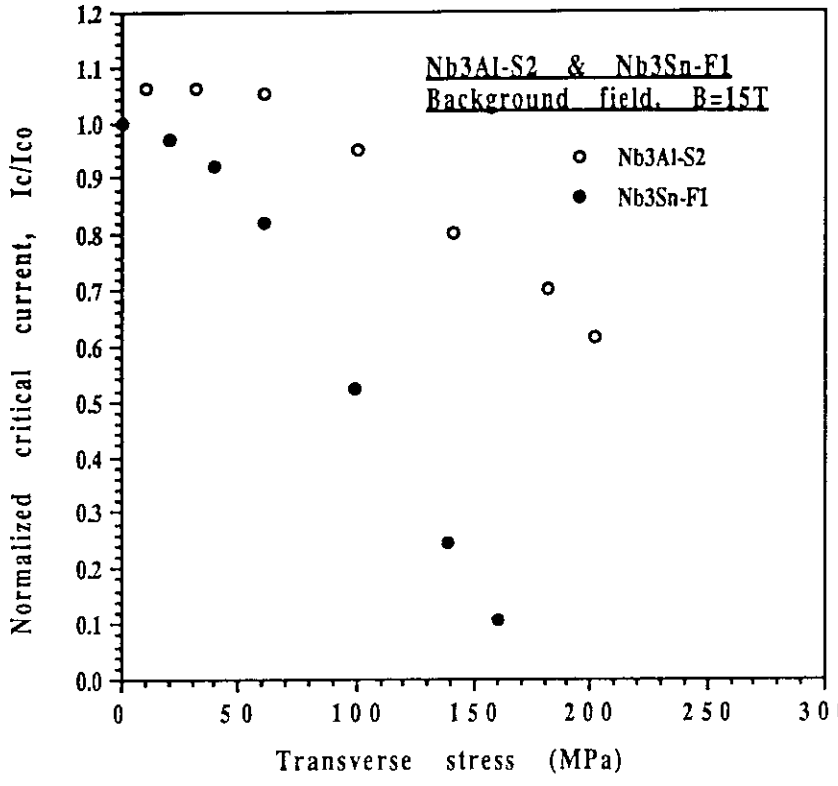

Fig. 6.15 I_c/I_{co} versus σ_t at 15T for samples Nb_3Sn-F1 and Nb_3Al-S2

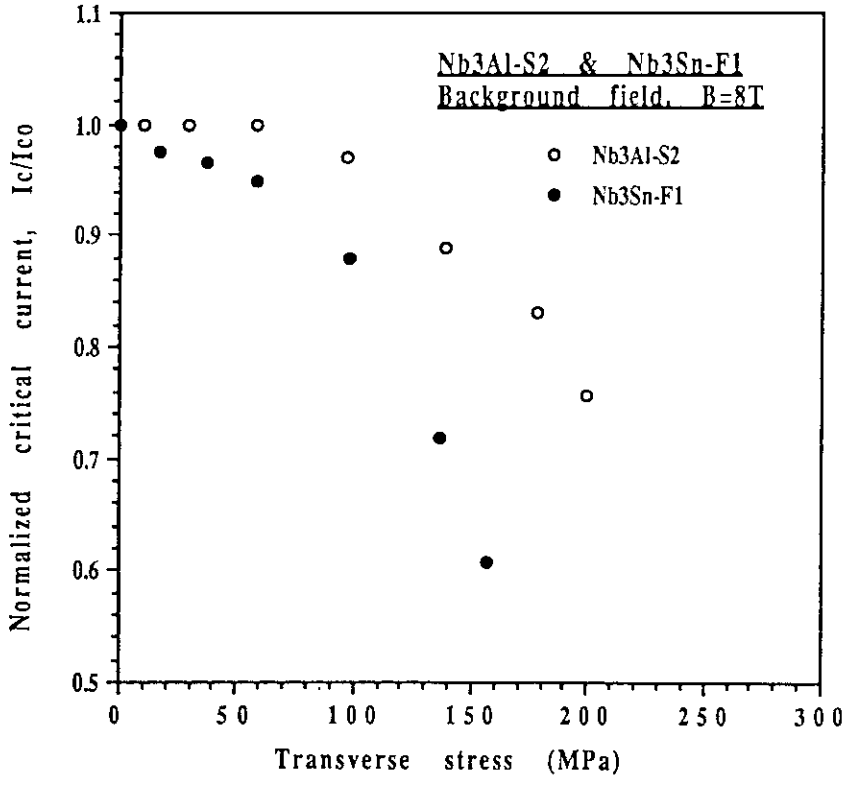

Fig. 6.16 I_c/I_{co} versus σ_t at 8T for samples Nb_3Sn-F1 and Nb_3Al-S2

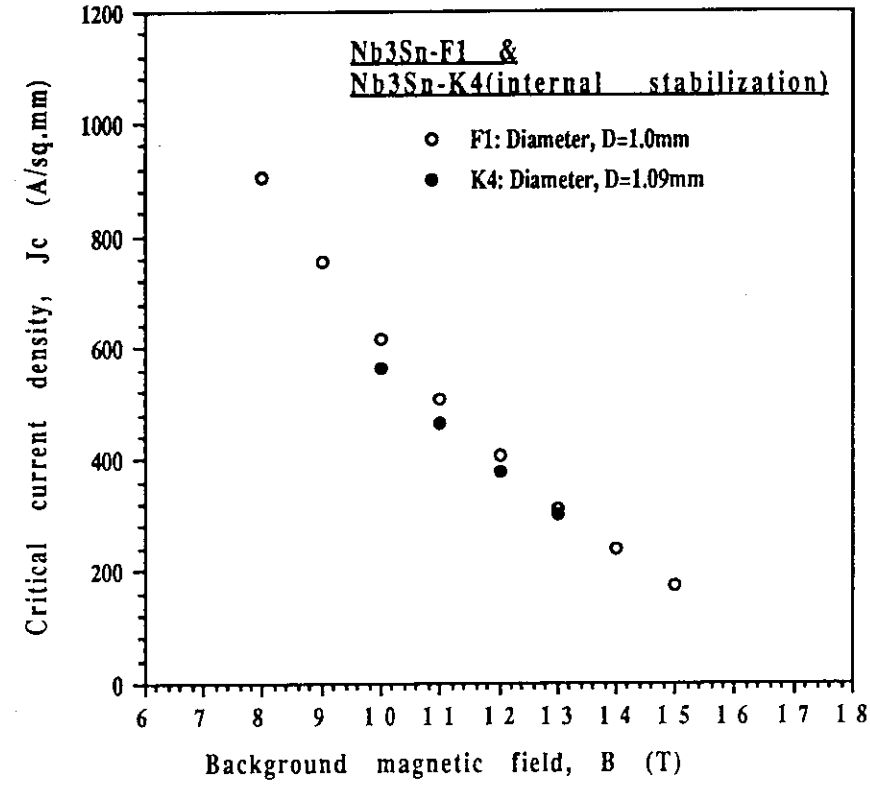

Fig. 6.17 J_c versus B for samples Nb_3Sn-F1 and Nb_3Sn-K4

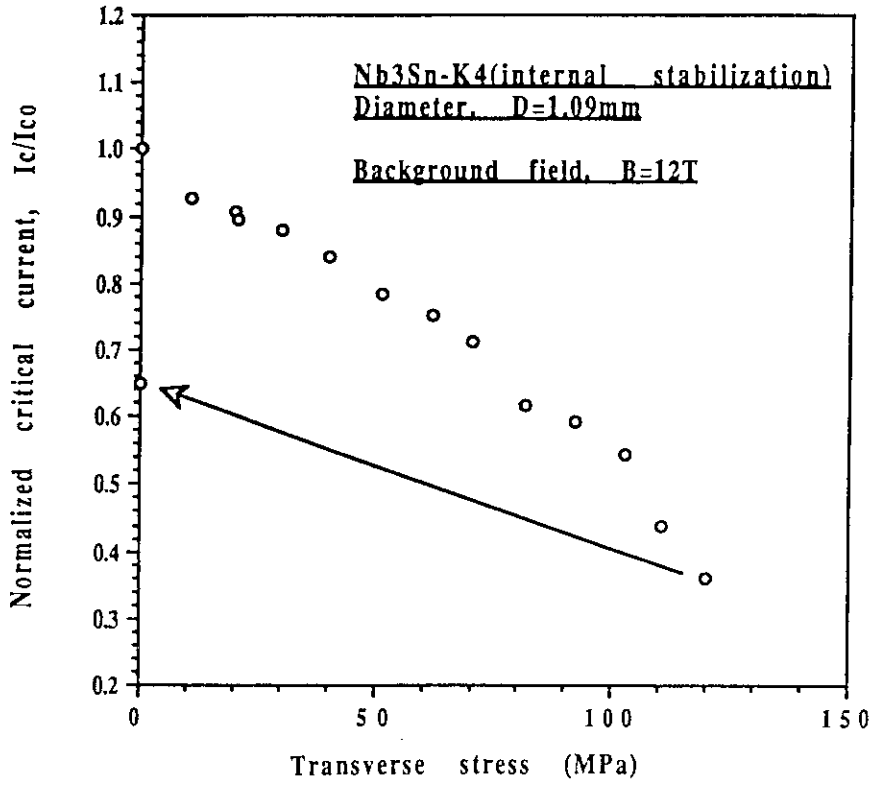

Fig. 6.18 I_c/I_{co} versus σ_t at 12T for sample Nb_3Sn-K4

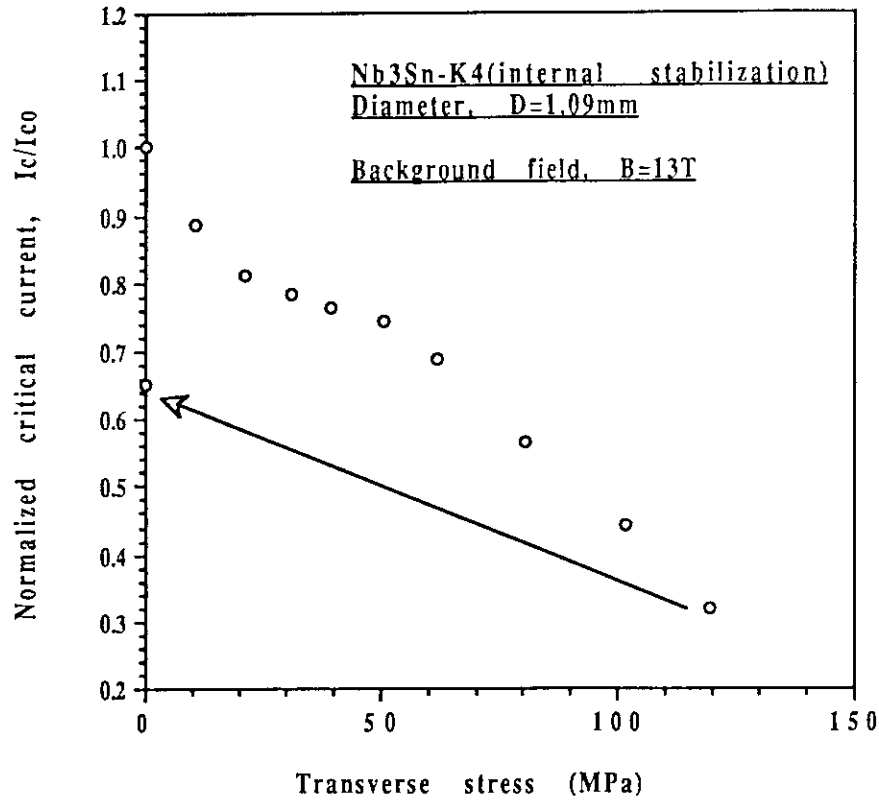

Fig. 6.19 I_c/I_{co} versus σ_t at 13T for sample Nb_3Sn-K4

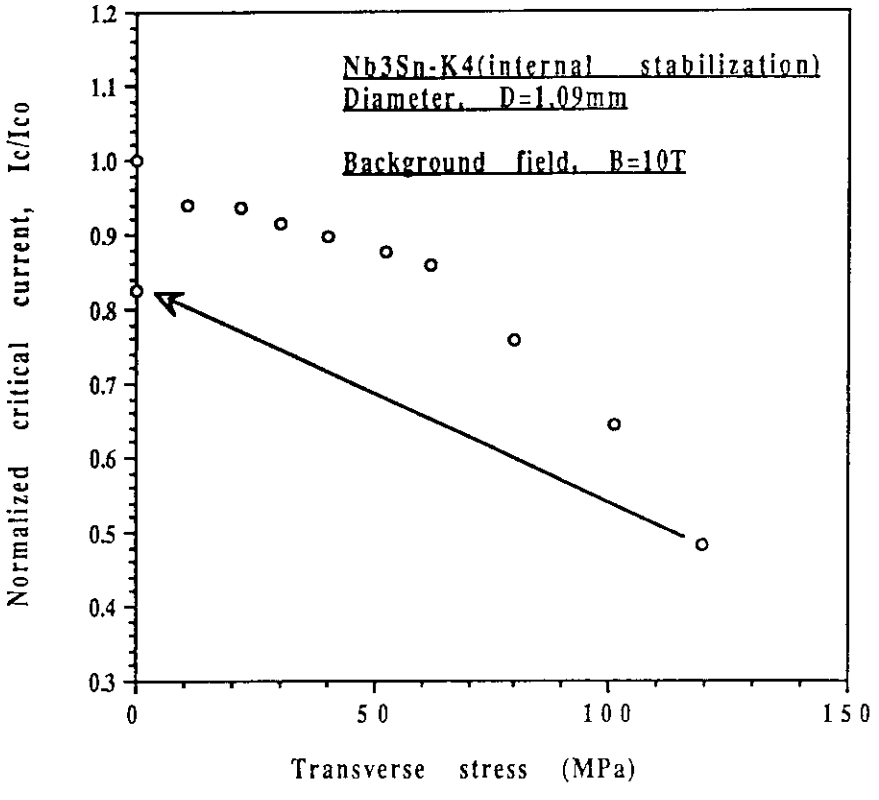

Fig. 6.20 I_c/I_{co} versus σ_t at 10T for sample Nb_3Sn-K4

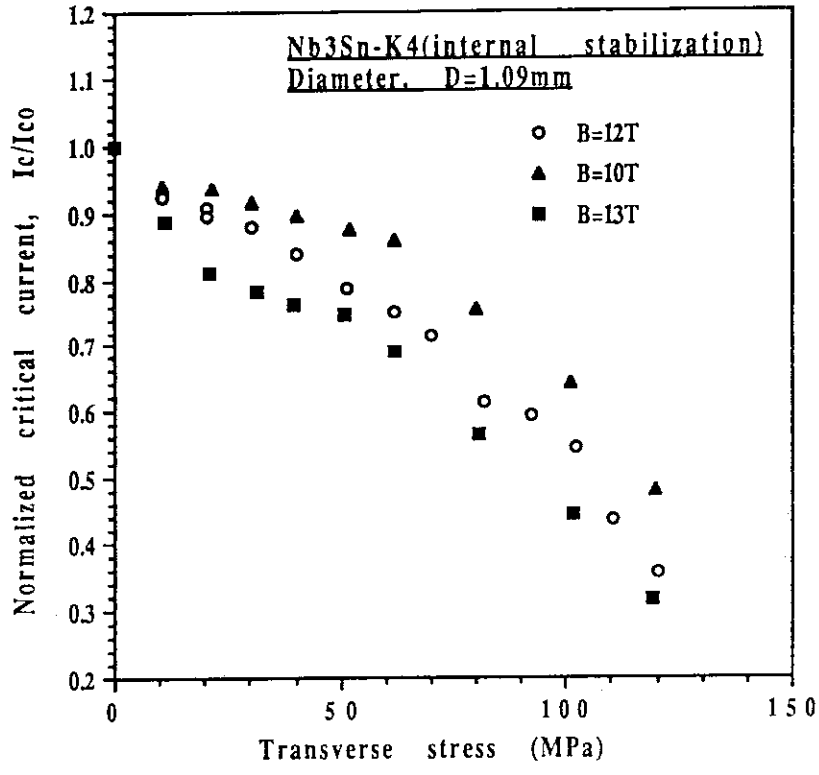

Fig. 6.21 I_c/I_{co} versus σ_t at different fields for sample Nb_3Sn-K4

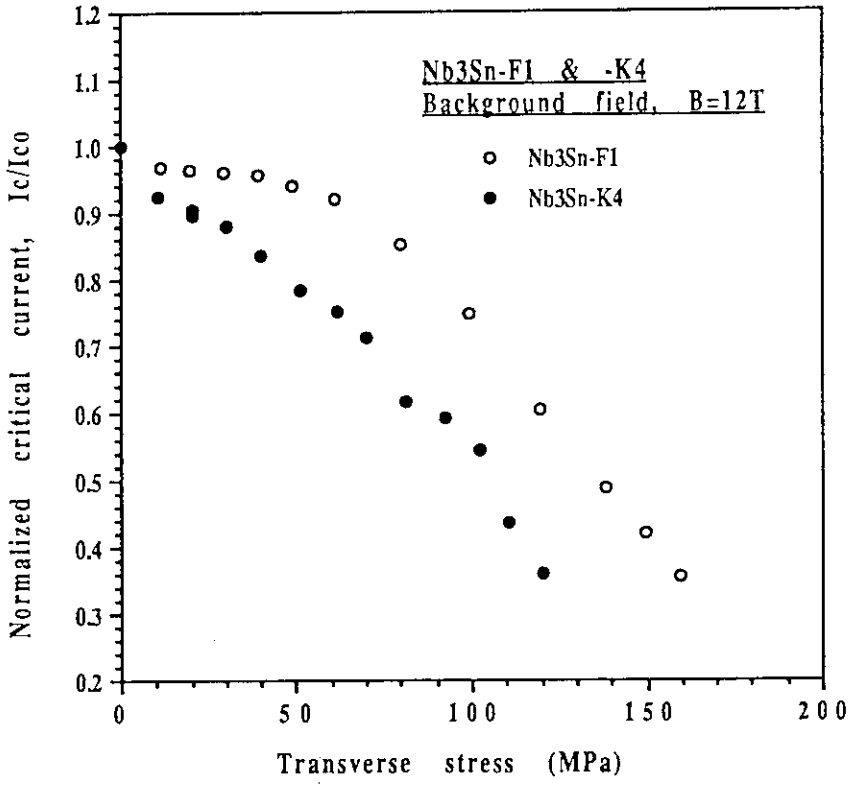

Fig. 6.22 I_c/I_{co} versus σ_t at 12T for samples Nb_3Sn-F1 and Nb_3Sn-K4

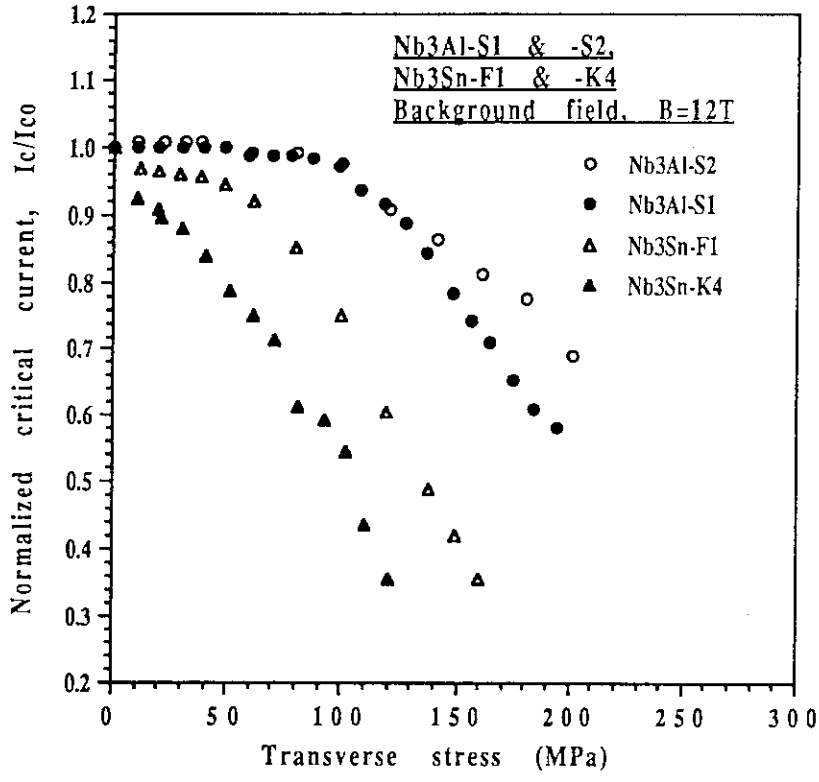

Fig. 6.23 I_c/I_{co} versus σ_t at 12T for all tested samples

7. Conclusions

We tested the transverse stress sensitivity of the critical current of four samples, two jelly-roll Nb_3Al samples and two Ti-alloyed bronze process Nb_3Sn samples. The aim of our work was to compare the transverse sensitivity of Nb_3Al wires to that of Nb_3Sn, primarily at 12T but also at other magnetic fields.

Without taking precompression effects due to differential thermal contraction into consideration, the Nb_3Al wires at 12T were considerably less sensitive to transverse stress than the Nb_3Sn wires, at high transverse stresses by as much as a factor of ~3-4. Nevertheless, the critical current densities attained at 12T by the fromer were lower by as much as 40-50 percent than those of the latter. It is clear that there is room for development in Nb_3Al wires fabricated by the jell-roll process, in order to increase their current densities at high fields. As soon as that is accomplished, possibly in a matter of a few years, the intrinsic superiority of Nb_3Al wires over Nb_3Sn with regard to transverse stress, or stress in general, should establish them as useful superconductors for large-scale, high-field applications.

8. Recommendations and future work

Our apparatus for testing the transverse sensitivity of Nb_3Al and Nb_3Sn wires performed remarkably well, despite the unfortunate malfunction of the servo motor and the replacement of it by the manual jack-system. However there is one area where it would benefit from improvement: the rigid attachment of the samples to the current leads. The current leads in our apparatus where stationary, therefore it was possible that an imperfectly installed sample could be stressed in ways other than purely transversely, with possible irreversible internal damage done to it. Moreover, during cooldown, differential thermal contraction between the sample and the supporting structure could have imparted axial stresses to a sample in addition the welk-known internal ones, altering the pre-experimental internal strain-state of the sample which, at least in Nb_3Sn, can have significant consequences. A recommendation therefore is to redesign the apparatus to have movable current leads, to avoid damage on the sample during transverse compression and to reduce the possibility of residual stresses superimposed over the ones internal to the sample during cooldown. The installation of movable current leads could eliminate the encountered drop in the I_c of the two Nb_3Sn samples, as well as the encountered enhancement at high fields of the critical current of the Nb_3Al samples.

A recommendation with regard to future testing would be to establish an environment where the directions of the background magnetic field, the current, and the transverse load are all mutually perpendicular. This was not the case during our experiments, nevertheless this should not have had any consequences on round samples such as ours. It could have had consequences on flat samples, especially ones with highly aspected cross-sections.

An area of work which we shall be undertaking in the near future is to correlate the transverse-stress-induced I_c-degradation of the Nb_3Al and Nb_3Sn test-samples to the degradation of their upper critical magnetic field. Presently we do not have critical current data for sufficiently high magnetic fields, and this precludes the accurate formulation of a scaling law.. We intend to formulate a model by which to calculate the internal triaxial strain-state in Nb_3Al and Nb_3Sn wires, as a result of transverse compression.

Acknowledgements

I would like to express my warmhearted appreciation to the head of JAERI's superconducting magnet laboratory Shimamoto Susumu, and to my advisor at MIT Iwasa Yukikazu, for affording me the opportunity to live and study in Japan. Also to Tsuji Hiroshi, to my advisor Ando Toshinari, and to my teacher, co-worker, and friend Takahashi Yoshikazu. Finally to everyone else in the superconducting magnet laboratory, for making my stay in Japan a unique and memorable experience, Nishi Masataka, Nakajima Hideo, Koizumi Kouichi, Tada Eisuke, Yoshida Kiyoshi, Okuno Kiyoshi, Kato Takashi, Isono Takaaki, Hiyama Tadao, Oshikiri Masayuki, Kawano Katsumi, Itoh Noboru, Nisugi Hikaru, Onawa Yasuko, Yoshida Kazuko, and Sugimoto Makoto, Ishida Hideaki, Yoshida Jun, Kamiyauchi Youichi, Kawagoe Eiji, and Konno Masayuki.

Special thanks to Sumitomo Electric Industries, Furukawa Electric Industires, and Kobe Steel Ltd., purveyors of the Nb_3Al and Nb_3Sn samples. Also to the U.S. Department of Energy, for sponsoring my graduate work, and to the MIT-Japan program, for their financial support and their useful instruction on the ways of Japan.

References

[1] M.N. Wilson, Superconducting Magnets, Oxford University Press, New York, 1983.

[2] K.K. Chawla, Composite Materials - Science and Engineering, Springer-Verlong New York Inc., 1987.

[3] T.A. Painter, *AC Loss Time Constant Measurement on Nb_3Al and NbTi Multifilamentary Superconductors*, JAERI-M 88-040, 1988, p.5.

[4] M. Suenaga, W.B. Sampson, and T.S. Luhman, *Fabrication Techniques and Properties of Multifilamentary Nb_3Sn Conductors*, IEEE Transactions on Magnetics MAG-17, 1981, p.646.

[5] M. Suenaga and W.B. Sampson, Applied Physics Letters 20, 1972, p.443.

[6] E.W. Howlett, U.S. Pat. 3,728,165 (Filed Oct. 19, 1970); Great Britain Pat. 52,623/69 (Filed Oct. 27, 1969).

[7] A.R. Kaufmann and J.J. Pickett, Bull.Am.Phys.Soc. 15, 1970, p.833.

[8] K. Tachikawa, International Cryogenics Engineering Conference, Berlin, W. Germany, 1970.

[9] K. Tachikawa, *Processing of Nb_3Al and Other Emerging Superconductors*, Advances in Cryogenic Engineering Materials 32, 1986, p.1049.

[10] Y. Hashimoto, K. Yoshizaki, and M. Tanaka, Procedings of the 5th International Cryogenics Engineering Conference, Kyoto, Japan 1974, p.332.

[11] K. Yoshizaki, M. Wakata, S. Miyashita, F. Fujiwara, O. Taguchi, M. Imaizumi, and Y. Hashimoto, *Improvements in Critical Current Densities of Internal Diffusion Process Nb_3Sn Wires by Additions of Third Elements*, IEEE Transactions on Magnetics MAG-21, No.2, 1988, p.301.

[12] R. Randall, J. Wong, D.W. Dies, B.J. Shaw, and M.R. David, IEEE Transactions on Magnetics MAG-11, 1975, p.291.

[13] Y. Koike, H. Shiraki, S. Murase, E. Suzuki, and M. Ichihara, Applied Physics Letters 29, 1976, p.384.

[14] S. Foner, C.L.H. Thieme, S. Purrahimi, and B.B. Schwartz, *Practical Processing of A15 Multifilamentary Wire from Powders: Nb_3Al and Nb_3Sn*, Advances in Cryogenic Engineering Materials 32, 1986, p.1,031.

[15] S. Foner, E.J. McNiff, Jr., T.H. Geballe, R.H. Willens, and E. Buehler, Physics 55, 1971, p.534.

[16] R.H. Willens, T.H. Geballe, A.C. Gossard, J.P. Maita, A. Menth, G.W. Hall, Jr., and R.R. Soden, Sodid State Commun. 7, 1969, p.837.

[17] E.A. Wood, V.B. Gompton, B.T. Matthias, and E. Corenzwit, Acta. Cryst. 11, 1958, p.604.

[18] K. Lo, J. Bevk, and D. Turnhull, Journal of Applied Physics 48, 1977, p.2597; Rapidly Quenched Metals, Third International Conference (Ed. B. Cantor) Vol.2, 1978, p.17.

[19] Hunt and Rahman, Zeit. für Metlkünde 59, 1968, p.701.

[20] R. Bormann, D.Y. Yu, R.H. Hammond, A. Marshall, and T.H. Beballe, Rapidly Quenched Metals (Eds. S. Steeb and H. Warlimont), North Holland, 1985, p.879.

[21] S. Ceresara, M.V. Ricci, N. Sacchetti, G. Sacerdoti, *Nb_3Al Formation at Temperatures Lower than 1000°C,* IEEE Transactions on Magnetics MAG-11, 1975, p.263.

[22] R. Bruzzese, N. Sacchetti, M. Spadoni, G. Barani, G. Donati, S. Ceresara, *Improved Critical Current Densities in Nb_3Al Based Conductors,* IEEE Transactions on Magnetics MAG-23, 1987, p.653; and references therein.

[23] C.B. Müller and E. Saur, Advances in Cryogenic Engineering Materials 8, 1963, p.574.

[24] W.B. Buehler and H.J. Levinstein, Journal of Applied Physics 36, 1965, p.3,856.

[25] D.S. Easton and R.E. Schwall, Applied Physics Letters 29, 1976, p.319.

[26] J.L. McDougall, Procedings of the International Cryogenics Engineering Conference, IPC Science and Technology Press 6, 1976, p.396.

[27] R.M. Scanlan, R.W. Hoard, D.N. Cornish, and J.P. Zbansnik, *Mechanical Properties of High-Current Multifilamentary Nb_3Sn Conductors,* Filamentary A15 Superconductors (Eds. M. Suenaga and A.F. Clark), Plenum Press, 1980, p.221.

[28] R.W. Hoard, R.M. Scanlan, and D.G. Hirzel, *MAXIMSUPER: A Computer Program to Assist in the Design of Multifilamentary Superconducting Composites,* Advances in Cryogenic Engineering Materials 26, 1980, p.578.

[29] J.L. Jorda, F. Flükiger, and J. Müller, Journal of Less Common Metals 75, 1980, p.227.

[30] R. Flükiger and W. Goldacker, *Physical Metallurgy and Critical*

Currents in Nb_3Al Multifilamentary Wires, Procedings of the 9th International Conference on Magnet Technology, Zürich Switzerland, September 9-13, 1985, p.553.

[31] W. Goldacker and R. Flükiger, *Calculation of Stress Tensors in Nb_3Sn Multifilamentary Wires*, Advances in Cryogenic Engineering Materials 34, 1988, p.561.

[32] W. Specking, W. Goldacker, and R. Flükiger, *Effect of Transverse Compression on I_c of Nb_3Sn Multifilamentary Wire*, Advances in Cryogenic Engineering Materials 34, 1988, p.569.

[33] W. Specking, F. Weiss, and R. Flükiger, *Effect of Transverse Compressive Stress on I_c up to 20T for Binary and Ta Alloyed Nb_3Sn Wires*, Procedings of the 12th Symposium on Fusion Engineering, Monterey, CA, U.S.A., IEEE Catalog No. 87, Ch.2507-2, 1987, p.365.

[34] J.W. Ekin, F.R. Fickett, and A.F. Clark, Procedings of the International Cryogenic Materials Conference (August 1975), Advances in Cryogenic Engineering Materials 22, 1977, p.449.

[35] J.W. Ekin, Applied Physics Letters 29, 1976, p.216.

[36] J.W. Ekin, Procedings of the International Cryogenic Materials Conference (August 1977), Advances in Cryogenic Engineering Materials 24, 1978, p.306.

[37] J.W. Ekin, *Strain Scaling Law and the Prediction of Uniaxial Bending Strain Effects in Multifilamentary Superconductors*, Filamentary A15 Superconductors (Eds. M. Suenaga and A.F. Clark), Plenum Press, New York, 1980, p.187.

[38] J.W. Ekin, *Strain Scaling Law for Flux Pinning in Practical Superconductors, Part 1: Basic Relationships and Application to Nb_3Sn Conductors*, Cryogenics, Nov. 1980, p.611.

[39] J.W. Ekin, *Mechanical Properties and Strain Effects in Superconductors*, Superconductor Materials Science (Eds. S. Foner and B.B. Schwartz), Plenum Press, New York, 1981, p.455.

[40] J.W. Ekin, *Strain Effects in Superconducting Compounds*, Advances in Cryogenic Engineering Materials 30, 1984, p.823.

[41] J.W. Ekin, *Effect of Transverse Compressive Stress on the Critical Current and Upper Critical Field of Nb_3Sn*, Journal of Applied Physics 62 (12), 1987, p.4829.

[42] J.W. Ekin, *Effect of Transverse Compressive Stress on multifilamentary Nb_3Sn Superconductors*, Advances in Cryogenic Engineering Materials 34, 1988, p.547.